NASA TECHNICAL MEMORANDUM

NASA TM X-3162

NASA TM X-3162

DOWNWIND HAZARD CALCULATIONS FOR SPACE SHUTTLE LAUNCHES AT KENNEDY SPACE CENTER AND VANDENBERG AIR FORCE BASE

Michael Susko, C. Kelly Hill, and John W. Kaufman

George C. Marshall Space Flight Center
Marshall Space Flight Center, Ala. 35812

NATIONAL AERONAUTICS AND SPACE ADMINISTRATION • WASHINGTON, D. C. • DECEMBER 1974

1. REPORT NO.	2. GOVERNMENT ACCESSION NO.	3. RECIPIENT'S CATALOG NO.
NASA TM X-3162		

4. TITLE AND SUBTITLE	5. REPORT DATE
Downwind Hazard Calculations for Space Shuttle Launches at Kennedy Space Center and Vandenberg Air Force Base	December 1974
	6. PERFORMING ORGANIZATION CODE M126
7. AUTHOR(S) Michael Susko, C. Kelly Hill, and John W. Kaufman	8. PERFORMING ORGANIZATION REPORT #
9. PERFORMING ORGANIZATION NAME AND ADDRESS	10. WORK UNIT NO.
George C. Marshall Space Flight Center Marshall Space Flight Center, Alabama 35812	11. CONTRACT OR GRANT NO.
	13. TYPE OF REPORT & PERIOD COVERED
12. SPONSORING AGENCY NAME AND ADDRESS	Technical Memorandum
National Aeronautics and Space Administration Washington, D.C. 20546	14. SPONSORING AGENCY CODE

15. SUPPLEMENTARY NOTES

Prepared by Space Sciences Laboratory, Science and Engineering

16. ABSTRACT

Presented in this report for several meteorological conditions, are the quantitative estimates of pollutant concentrations associated with the emission of the major combustion products (HCl, CO, and Al_2O_3) to the lower atmosphere during normal launches of the Space Shuttle at Kennedy Space Center and Vandenberg Air Force Base. The developmental experience in diffusion modeling was obtained from analyses of the dispersion procedure for effluents from the Scout-Algol III, Delta-Thor Telsat A, Titan III-C and E, and Saturn V. The NASA/ MSFC Multilayer Diffusion Model was used to obtain these calculations. In this report, results are presented for nine sets of typical meteorological conditions at Kennedy Space Center, including fall, spring, and a sea-breeze condition, and six sets at Vandenberg AFB. Outside an industrial area of 10 km at Kennedy Space Center and outside a similar distance at Vandenberg AFB, if a 10-min short term public limit of 4 ppm of HCl is applied (National Academy of Science/ National Research Council Committee on Toxicology), in none of the selected typical meteorological regimes studied (see Table 2 of text) was this 10-min limit exceeded. Also, scavenging of the exhaust cloud by precipitation was not considered and may result in increased concentration. Since all possible meteorological conditions that may exist during a Space Shuttle launch were not assessed in accordance with the Environmental Statement for the Space Shuttle Program issued in 1972, NASA intends to include in its operational procedures an assessment of downwind by-product concentration for the meteorological conditions expected at launch time.

17. KEY WORDS	18. DISTRIBUTION STATEMENT
Pollution Propellant Scavenging Space Shuttle Meteorology	Cat 12

19. SECURITY CLASSIF. (of this report)	20. SECURITY CLASSIF. (of this page)	21. NO. OF PAGES	22. PRICE
Unclassified	Unclassified	67	$4.25

ACKNOWLEDGMENT

This document presents the results of work performed by personnel of the Environmental Dynamics Branch (ES-43) of the Aerospace Environment Division, Space Sciences Laboratory, Marshall Space Flight Center, Alabama. Much credit must be given to Dr. Leonard L. DeVries of the Aerospace Environment Division who encouraged the preparation of this report and to Dr. J. Briscoe Stephens for his helpful comments. The authors are indebted to J. H. Scollard and Archie Jackson of the Data Systems Office. Messrs. R. K. Dumbauld, Jay R. Bjorklund, and James Bowers of the H. E. Cramer Company made significant contributions to the overall effort.

TABLE OF CONTENTS

TABLE OF CONTENTS (Concluded)

LIST OF ILLUSTRATIONS

LIST OF TABLES

DEFINITION OF SYMBOLS

Symbol		Meaning
F_C	=	continuous buoyancy flux term
	=	$\frac{gQ_F}{\pi\rho c_p T}$ (m^4/sec^3)
F_I	=	instantaneous buoyancy term
	=	$\frac{3gQ_I}{4c_p T\pi\rho}$ (m^4/sec^2)
FM	=	percentage by weight of pollutant material in the fuel from Table 1
H_L, H_S	=	respective heat contents of liquid and solid fuels (cal/g)
L	=	depth of the surface mixing layer (m)
M	=	molecular weight (g/mole)
P	=	ambient pressure (mb)
$P\{z_{TK}\}$	=	integral of the Gaussian probability function between minus infinity and the top of the Kth layer z_{TK}
	=	$P\left\{\frac{z_{TK} - z_{mI}}{\sigma}\right\}$
Q	=	total weight of exhaust products in the stabilized exhaust cloud
	=	$(Q_R)\ (t_R\{z_{mI}\})\ (FM)\ (g)$
Q_F	=	rate of heat released by burning fuel
	=	$H_L \cdot W_L + H_S \cdot W_S$ (cal/sec)

DEFINITION OF SYMBOLS (Continued)

Symbol		Meaning
Q_I	=	effective heat released (cal)
Q_K	=	source strength in units of mass per unit depth of the Kth layer (g/m)
T	=	ambient air temperature (°K)
W_L, W_S	=	respective fuel expenditure rates, liquid and solid fuel (g/sec)
z	=	height above ground of any selected layer (m)
c_p	=	specific heat of air at constant pressure 0.24 cal/°K g
g	=	gravitational acceleration (9.8 m/sec^2)
r_R	=	initial cloud radius at the surface (m)
$s = \frac{g}{T} \frac{\partial \Phi}{\partial z}$	=	stability parameter (1/sec^2)
t^*	=	time of layer breakdown (sec)
t_H	=	time after ignition required for the cloud to reach the stabilization height (sec)
t_R	=	time after ignition (sec)
t_{sI}	=	time required for the cloud to achieve stabilization in an adiabatic atmosphere (sec)
$t_R z_{mI}$	=	time required for the vehicle to reach the height z_{mI} of maximum rise of the ground cloud (sec) [obtained from equation (1)]
$\bar{u}$	=	mean wind speed (m/sec)
z	=	height of stabilized cloud (m)

DEFINITION OF SYMBOLS (Continued)

Symbol		Meaning
z'	=	midpoint of the Kth layer
	=	$\left(z_{BK} + z_{TK}\right)/2$ (m)
z_{BK}	=	height of the base of the Kth layer (m)
z_{BL}	=	height of the base of the Lth layer (m)
z_L	=	height in the Lth layer at which the concentration is calculated (m)
z_{mC}	=	maximum height of cloud rise for a continuous source (m)
z_{mI}	=	maximum rise for an instantaneous source (m)
z_{TK}	=	height of the top of the Kth layer (m)
z_{TL}	=	height of the top of the Lth layer (m)
z_R	=	altitude above the pad (m)
γ_C	=	entrainment constant (continuous) (dimensionless)
γ_I	=	entrainment constant (instantaneous) (dimensionless)
σ	=	standard deviation of the concentration distribution of the stabilized ground cloud (m)
σ_{xK}	=	standard deviation of the alongwind concentration distribution in the Kth layer at distance x (m)
σ_{xLK}	=	standard deviation of the alongwind concentration distribution in the Lth layer for the source originating in the Kth layer (m)
$\sigma_{xo}\{K\}$	=	standard deviation of the alongwind concentration distribution in the Kth layer at cloud stabilization (m)

DEFINITION OF SYMBOLS (Concluded)

Symbol		Meaning
$\sigma_{yo}\{K\}$	=	standard deviation of the crosswind concentration distribution in the Kth layer at cloud stabilization (m)
$\sigma_{zo}\{K\}$	=	standard deviation of the vertical concentration distribution in the Kth layer at cloud stabilization (m)
σ_{yK}	=	standard deviation of the crosswind concentration distribution in the Kth layer at distance x (m)
σ_{yLK}	=	standard deviation of the crosswind concentration distribution in the Lth layer for the source originating in the Kth layer (m)
σ_{zLK}	=	standard deviation of the vertical concentration distribution in the Lth layer for the source originating in the Kth layer (m)
ρ	=	density of ambient air (g/m^3)
$\frac{\partial \Phi}{\partial z}$	=	vertical gradient of ambient potential temperature (°K/m)
χ_p	=	peak or centerline concentration (ppm)

TECHNICAL MEMORANDUM X-3162

DOWNWIND HAZARD CALCULATIONS FOR SPACE SHUTTLE LAUNCHES AT KENNEDY SPACE CENTER AND VANDENBERG AIR FORCE BASE

SUMMARY

The NASA/MSFC Multilayer Diffusion Model is used to predict the dispersion from the rocket motors of the Space Shuttle at Kennedy Space Center and Vandenberg Air Force Base. The analysis of the dispersion of the rocket exhaust effluents is for the nine meteorological regimes at Kennedy Space Center (KSC) and six at Vandenberg Air Force Base (VAFB). It is concluded that outside the Kennedy Space Center industrial area of 10 km and outside a similar distance at Vandenberg Air Force Base, if a 10-min short term public limit of 4 ppm of HCl is applied (NAS/NRC Committee on Toxicology), in none of the typical selected meteorological cases studied was the 10-min limit exceeded. From related climatological studies meteorological conditions will exist at both launch sites that will constrain the shuttle launches. As an example, one case at KSC had a 5 ppm average concentration for a 10-min period at 2 km and 1.9 at 10 km distance from the launch pad. Also, scavenging of the exhaust cloud by precipitation was not considered and may result in increased concentration.*

INTRODUCTION

Purpose and Scope

The purpose of this technical memorandum is to provide quantitative estimates of pollutant concentrations associated with the emission of three major combustion products, HCl, CO, and Al_2O_3, to the lower atmosphere during normal launches at Kennedy Space Center and Vandenberg Air Force Base. These estimates are provided by the Marshall Space Flight Center to assist the National Aeronautics and Space Administration in assessing the environmental impact of Space Shuttle launch operations. Attention has been focused on calculations of pollutant concentrations near ground level at various downwind distances. Only calculations for normal launches are presented in this report.

---

*Anon. Potential Tropospheric Exhaust Cloud Constraint and Shuttle Launch Delay Risk Assessment: Internal Report by Aerospace Environment Division, Space Sciences Laboratory, NASA-Marshall Space Flight Center, August 1974.

The pollutant concentration calculations have been made by using the computerized NASA/MSFC Multilayer Diffusion Models [1, 2] in conjunction with appropriate emissions data for the Space Shuttle solid propellant engines and with meteorological data for a number of selected situations characteristic of each launch site. In this report, results are presented for nine sets of meteorological conditions at Kennedy Space Center and six sets at Vandenberg Air Force Base.

Fuel Properties and Vehicle Rise Data

Characteristic fuel properties used in the concentration calculations are given in Table 1 and are principally based on data from the "Mission 1 Ascent Trajectories (MCR 200R1 Configuration)" dated June 18, 1973.

$$Q_F = W_s \cdot H_s + W_L \cdot H_L \quad , \tag{1}$$

where

$$(Q_F) = \text{total heat output} = (W_S)\ 9.45126 \times 10^6 \cdot (H_S)\ 6.91 \times 10^2$$

$$+ (W_L)\ 1.53116 \times 10^6 \cdot (H_L)\ 5.00 \times 10^2 \quad ,$$

$$Q_F = 7.2964 \times 10^9 \text{ cal/sec} \quad .$$

However, it is assumed that 1.26×10^3 kg/sec of water would be used to cool the launch pad and that all the water is vaporized by the engine. This results in a heat loss (Q_L) of 7.74×10^8 cal/sec. The effective heat used in the plume rise calculation is

$$Q_E = Q_F - Q_L \quad . \tag{2}$$

$$(Q_E) \text{ effective heat} = (Q_F)\ 7.29640 \times 10^9 - (Q_L)\ 7.74 \times 10^8$$

$$Q_E = 6.52240 \times 10^9 \text{ cal/sec} \quad .$$

The liquid engine does not release any of the three pollutants, HCl, CO, and Al_2O_3.

The altitude-time curve for the Space Shuttle is also required to calculate the rise of the ground cloud of exhaust products. A logarithmic least squares regression curve was fitted to the time height data for the first 40 sec of flight yielding the expression

$$t_R = 0.672341Z^{0.48284} \quad , \tag{3}$$

where t_R is time in seconds and Z is in meters. For convenience, Figure 1 shows a plot of vehicle altitude versus time calculated from equation (3).

Organization of the Report

The following section contains a description of the cloud rise calculations for the models. Cloud dimensions as vertical distributions of exhausts are discussed in the third section. A description of the MSFC Multilayer Diffusion Model used in the calculations of concentrations downwind from the launch is presented in the fourth section. The last section describes the results of the calculations at KSC and VAFB.

Appendix A contains a derivation of the plume rise equations and Appendix B contains a description of the procedures used in specifying the source and meteorological inputs. Appendix C includes the input parameters for the NASA/MSFC Multilayer Diffusion Model, and the toxicity criteria are given in Appendix D.

CLOUD RISE CALCULATIONS

Normal Launches

The burning of rocket engines during normal launches results in the formation of a cloud of hot exhaust products which subsequently rises and entrains ambient air until an equilibrium with ambient conditions is achieved. Experience in predicting the buoyant rise [3 - 14] from normal launches of

solid-fueled vehicles indicates the rise is best predicted using a cloud rise model for instantaneous sources. For solid-fueled vehicles residence times near the pad are relatively short.

Each of the models for cloud height is subdivided into two categories to account for the atmospheric temperature lapse rate. The model assumes that the atmosphere is either quasi-adiabatic or stable. Here the quasi-adiabatic is where the adiabatic atmosphere is the limit, which means that the potential temperature difference $(\Delta\theta)$ is zero or less, where the potential temperature difference is given by $\Delta\theta = \theta_{\text{max cloud height}} - \theta_{\text{surface}}$. If this potential temperature difference is positive, then the atmosphere is stable. Since in most cases of interest there will be an inversion layer present, the stable cloud rise formula is the normally utilized relation [15, 16].

Cloud Rise Models

The maximum rise z_{mI} for an instantaneous source as given by the expression in a stable atmosphere is given by

$$z_{mI} = \left[\frac{8F_I}{\gamma_I^3 s} + \left(\frac{r_R}{\gamma_I}\right)^4\right]^{1/4} - \frac{r_R}{\gamma_I} \quad , \tag{4}$$

whereas, the maximum cloud rise z_{mI} downwind from an instantaneous source in an adiabatic atmosphere is given by

$$Z_{mI} = \left[\frac{2F_I t_{SI}^2}{\gamma_I^3} + \left(\frac{\gamma_R}{\gamma_I}\right)^4\right]^{1/4} - \frac{\gamma_R}{\gamma_I} \quad . \tag{5}$$

In deriving equation (4), it is assumed that the initial upward momentum imparted to the exhaust gases by reflection from the ground surface and launch pad hardware is insignificant in comparison with the effect of thermal buoyancy. Based on limited experience in predicting cloud rise from launches at

Vandenberg Air Force Base, this assumption appears to be justified. The time required for the cloud to reach the stabilization height is given by the expression

$$t_H = \frac{\pi}{s^{1/2}} \quad . \tag{6}$$

In calculating z_{mI} from equation (5), the instantaneous heat released Q_I is obtained from the relationship

$$Q_I = Q_F \, t_R\{z_{mI}\} \quad . \tag{7}$$

An inspection of the equations given above reveals an interdependence between the calculated maximum cloud rise z_{mI}, the height over which the potential temperature gradient $\partial\Phi/\partial z$ is measured, and the value of $t_R\{z_{mI}\}$ used in obtaining Q_I. Thus, the final value of maximum cloud rise must be found through iteration of equations (4) or (5). The height over which $\partial\Phi/\partial z$ is measured and the time $t_R\{z_m\}$ are thus made consistent with the value of z_{mI} calculated from the model.

It should be noted that the height predictions for the cloud rise assume uniform potential temperature gradients over the atmospheric region in which the equations are applied. If a discontinuous atmospheric environment exists, relative to that over the launch site, as the exhaust cloud moves downwind and develops, then significant variation in the potential temperature gradient (and cloud rise) may occur unless this is taken into consideration. This can occur in regions of geographic discontinuities such as the land-water interface at the Kennedy Space Center area. If adequate measurements of the atmospheric structure exist, then the appropriate inputs can be made into the cloud rise prediction equations.

CLOUD DIMENSIONS AND VERTICAL DISTRIBUTION OF EXHAUST PRODUCTS

Source inputs required for the diffusion model calculations include the stabilization height of the exhaust cloud and cloud dimensions, as well as the vertical distribution of exhaust products in the stabilized cloud. The calculation of the stabilization height z_m was described previously. The calculation of the dimensions of the stabilized cloud and the vertical distribution of exhaust products is described below.

Dimensions of the Exhaust Cloud at Stabilization

The general formula used to calculate the radius of the stabilized cloud at height z is given by the expression

$$r\{z\} = \begin{cases} \gamma z & ; \quad z \leq z_m \\ \gamma\,(2z_m - z) \geq 200\ \text{m} & ; \quad z \geq z_m \end{cases} \quad , \tag{8}$$

where

$$\gamma = (\gamma_I) = 0.64 \quad .$$

Note that for $z > z_m$, the minimum radius of the stabilized cloud is set equal to 200 m.

The cloud is assumed to be symmetrical about a vertical axis through the cloud centroid. The alongwind and crosswind source dimensions of the cloud in each of the layers are calculated under the following assumptions:

- The distribution of exhaust products within the cloud is Gaussian in the plane of the horizon.
- The concentration of exhaust products at a lateral distance of 1 radius from the cloud vertical axis is 10 percent of the concentration at the cloud axis.

The alongwind and crosswind source dimensions required for input to the MSFC Diffusion Models are defined for each layer by

$$\sigma_{xo}\{K\} = \sigma_{yo}\{K\} = \left\{ \begin{array}{ll} \gamma z/2.15 & ; \quad z \leq z_m \\ \\ \gamma(2z_m - z)/2.15 \geq 93 \text{ m} & ; \quad z \geq z_m \end{array} \right\} \quad , \qquad (9)$$

where

z' = midpoint of the Kth layer

$$= (z_{BK} + z_{TK})/2 \quad .$$

The quantities z_{TK} and z_{BK} are, respectively, the height of the top and base of the Kth layer.

The corresponding vertical source dimension for each layer was calculated from the expression

$$\sigma_{zo}\{K\} = (z_{TK} - z_{BK})/\sqrt{12} \quad . \qquad (10)$$

Equation (10) applies to a rectangular material distribution which has been assumed to apply along the vertical in the Kth layer.

Calculation of the Vertical Source Strength Distribution in the Stabilized Exhaust Cloud

The fraction of material by weight in each of the K layers, $F\{K\}$, for the launches was calculated from the expression

$$F\{K\} = \begin{cases} Q\,P\{z_{TK}\} & ;\ K = 1 \\ Q(P\{z_{TK}\} - P\{z_{BK}\}) & ;\ K > 1 \end{cases} \quad . \qquad (11)$$

$P\{z_{BK}\}$ is the integral of the Gaussian probability function between minus infinity and the base of the Kth layer, z_{BK}, and is equal to $P\{z_{BK} - z_{mI}/\sigma\}$. σ is equal to $\gamma\{z = z_{mI}\}/2.15$.

The MSFC Diffusion Model described in the next section requires that source strength in each of the K layers be specified per unit height. Since the desired concentration units for HCl and CO are parts per million, the complete expression for the source strength model input for the Kth layer is

$$Q_K = \left[\frac{F\{K\}}{(z_{TK} - z_{BK})}\right]\left(\frac{10^3\ mg}{g}\right)\left(\frac{22.4}{M}\right)\left(\frac{T\{z_R\}}{273.16}\right)\left(\frac{1013.2}{P\{z_R\}}\right) \quad . \qquad (12)$$

For Al_2O_3, the desired concentration units are milligrams per cubic meter and the complete expression for source strength in the Kth layer is

$$Q_K = \frac{F\{K\}}{(z_{TK} - z_{BK})}\left(\frac{10^3\ mg}{g}\right) \quad . \qquad (13)$$

Equations (11), (12), and (13) were used to obtain the model input values of Q_K for the various meteorological regimes.

NASA/MSFC MULTILAYER DIFFUSION MODEL

The spatial description, in terms of concentration and dosage, of the dispersive transport of effluents from a discrete source is afforded by the NASA/MSFC Multilayer Diffusion Model. Specifically, this application of the model is for the prediction of toxicity distribution associated with the rocket exhaust effluents emitted during the launch of a space vehicle in order to assess

the resulting environmental impact. The dispersive description accorded by the Multilayer Diffusion Model is initiated at the point where the cloud of effluents reaches thermodynamic equilibrium with the environment, and therefore depends strongly on the kinematic and thermodynamic profiles of the atmospheric conditions along with a knowledge of the exhaust effluents present in the cloud.

The initial considerations in this section are given to the techniques of establishing the spatial location of the ground cloud equilibrium. Secondly, a general discussion of the Lagrangian dispersion of a point source is given. The final discussion in this section explains how the Multilayer Diffusion Model incorporates the general diffusion description to account for the two stages of exhaust emission and accounts for the environmental effects. The significant mathematical expressions supporting these discussions have been included in Appendices A, B, and C.

Altitude of Cloud Equilibrium

The effluent cloud rise relations are employed to determine the altitude at which the ground cloud reaches equilibrium with the environment. The importance of this location is that it serves as the origin of the dispersive description. This equilibrium point is chosen as the origin in order to eliminate complex thermodynamic considerations and to limit the problem solely to kinematics.

The burning of rocket engines results in the formation of a cloud of hot exhaust products which subsequently rises and entrains ambient air until an equilibrium with ambient conditions is reached. For normal launches, this cloud is formed principally by the forced ascent of hot turbulent exhaust products that have been deflected laterally and vertically by the launch pad hardware and the ground surface. The height at which this ground cloud stabilizes is determined by the vehicle type and atmospheric stability. The vehicle type determines whether a continuous or instantaneous source model is required. In the instantaneous source model, spherical entrainment is assumed; that is, the entrained ambient air enters the exhaust cloud uniformly from all directions. In the continuous source model, cylindrical entrainment is assumed; that is, the entrained ambient air enters the cloud uniformly only on the sides of the cylinder and not the ends.

The generalized dosage model for a nearly instantaneous source is defined by the product of four modular terms:

$$\text{Dosage} = \{\text{Peak Dosage Terms}\} \times \{\text{Lateral Term}\} \times \{\text{Vertical Term}\} \times \{\text{Depletion Term}\} \quad .$$

Thus, the mathematical description for the concentration and dosage models permit flexibility in application to various sources and for changing atmospheric parameters while always maintaining a rigorous mass balance.

Two obvious differences exist. First, the peak concentration term refers to the concentration at the point $x, y = 0, z = H$ (where x is the wind direction and H is any height) and is defined by the expression

$$\frac{Q}{(2\pi)^{3/2} \sigma_x \sigma_y \sigma_z} \quad , \tag{14}$$

where Q is the source strength and σ_i is the standard deviation ot the concentration distribution in the ith direction. The peak dosage term is given by

$$\frac{Q}{2\pi \bar{u} \sigma_y \sigma_z} \quad , \tag{15}$$

where $\bar{u}$ is the mean wind speed. The second difference between these models is that the concentration contains a modular alongwind term to account for downstream temporal effects not considered in the dosage model. The alongwind term affords an exponential decay in concentration as a function of: cloud transit time, concentration distribution, and the mean wind speed.

The lateral term, which is common to both models, is another exponential decay term and is a function of the Gaussian spreading rate and the distance laterally from the mean wind azimuth. The vertical term, again common to both models, is a rather complex decay function since it contains a multiple reflection term for the point source which stops the vertical cloud development at the top of the mixing layer and eventually changes the form of the vertical

concentration distribution from Gaussian to rectangular. The last modular in both models is the depletion term. This term accounts for the loss of material by simple decay processes, precipitation scavenging, or gravitational settling.

The Description of the Models in the NASA/MSFC Multilayer Diffusion Model

The normal launch environment will usually involve an atmospheric structure comprised of several horizontal meteorological layers with distinctive wind velocity, temperature, and humidity regimes between the surface and a 5-km altitude. Large horizontal spatial variation in these meteorological parameters may also occur in the surface layer as a consequence of changes in terrain or land-water interfaces, which is accounted for by the diffusion model. The general diffusion model for the concentration [equation (14)] and the dosage [equation (15)] assumes an expanding volume about a moving point of reference in a homogeneous environment [17 - 20].

To overcome the obvious shortcomings of the general diffusion model but to stay within the established bounds of classical fluid mechanics [21], a multiple layer concept is introduced to cope with the vertical and horizontal atmospheric gradients. Here, the general diffusion model is applied to individual horizontal layers in which the meteorological structure is reasonably homogeneous and independent of the neighboring layers. These layers have boundaries which are placed at points of major discontinuities in the vertical profiles of wind velocity, temperature, and humidity. Since the Multilayer Diffusion Model has imposed the general restriction of layer independence (no flux of particles or gases entering or leaving an individual layer), special provision must be made for spatial changes in the horizontal meteorology and for gravitational settling or precipitation scavenging. In addition, the type of source within a layer must be considered; that is, whether there is a ground cloud source or a plume cloud source.

The NASA/MSFC Multilayer Diffusion Model has six models (Fig. 2) which account for three categories of dispersive constraints: the source distribution, the environmental effects, and the depositional effects. This flexibility is required to deal with the stages of the development of the exhaust cloud and the complex, potentially varying, meteorological conditions. These models can be used alone to describe all the environmental layers or in superimposed combinations where variations in layer meteorology require different modeling. For the introductory overview, however, these combinations will not be considered. The primary output of all models is a mapping of the regimes of the concentration and dosage isopleths and centerline profiles for concentration and dosage.

The fundamental category of dispersive constraints is the source distribution. The two distributions are:

1. The elliptic-cylindrical source which assumes a two-dimensional Gaussian distribution in the x-y plane and a uniform distribution in the vertical direction.

2. The ellipsoidal source which assumes a three-dimensional Gaussian distribution.

Model 1 is for the elliptic-cylindrical source whose vertical expansion is constrained by the layer boundaries – thus it has only a two-dimensional expansion in the horizontal plane due to turbulence mising. This model is normally used to describe the rocket' s inflight plume cloud.

Model 3 is for the ellipsoidal source and is assumed to expand in all three dimensions as the effluents are propagated downstream. When the ellipsoidal source reaches the top of the mixing layer, the distribution of the constituents is reflected back into the expanding vertical distribution. On the other hand, that fraction not lost in surface deposition is also reflected back in a similar manner. After sufficient mixing, the ellipsoidal distribution becomes an elliptic-cylindrical distribution (Model 1). While Model 3 is normally used to describe the dispersion of the rocket' s ground cloud, it could be used to model upper air explosions. The formulation for Model 3 has been provided in Appendix B.

The second category is environmental effects. The two effects are:

1. No turbulence mixing in the upper atmosphere.

2. Changes in meteorological conditions as the constituents are transported downstream.

Model 2 is the same as Model 1 except it is assumed that there is no turbulent mixing. This implies that the exhaust material just meanders along the layer without dispersing. While Model 2 is not generally used, movies of rocket firings clearly show that under some special meteorological conditions this model is required. While the Multilayer Diffusion Model is general in applicability, it is specific in meteorological parameters and launch description.

Model 4 updates the diffusion model with changes in meteorological conditions and structure which can occur as the constituents propagate downstream. This model assumes that the vertical concentration of material has become

uniform throughout each layer when a step-change in the meteorological conditions is introduced, resulting in the destruction of the original layer boundaries and the formation of new layer boundaries. The concentration fields which exist at this time are treated as new sources. In those new layers which now comprise more than one old layer, the old concentration is mapped as two independent concentration sources and then superimposed for the resulting concentration and dosage mappings.

The third category of dispersive contraints includes the deposition due to: (1) precipitation scavenging and (2) gravitational settling.

Model 5 accounts for precipitation scavenging. An example of where Model 5 must be used is in solid rocket launches during the occurrence of rain, because the HCl will be scavenged by the rain. Model 6 describes the ground deposition due to gravitational settling of particles or droplets. Wind shears are incorporated in this model to account for the effect of the settling velocity of the particulate matter. There are two forms for the source in this model; namely,

1. The source that extends vertically through the entire layer with a uniform distribution — this is the same source model as used with Models 1 and 2.

2. A volume in the Kth layer — this is the same source model as used with Model 3.

Model 6 is very important in the analysis of the settling of Al_2O_3 particles released in solid rocket firings.

The treatment of cold spills and fuel leaks that occur near ground level requires a continuous source, but the models that have been considered so far are for discrete sources; therefore, the models must be adapted for the use in predicting concentration-dosage levels downwind from continuous sources.

The layer of the environment influenced by the ground-level spills and leaks can be treated as homogeneous; therefore, the general formulas for concentration and dosage [equations (14) and (15)] presented in the initial discussion would be applicable if spills and leaks are treated as continuous sources. To visualize this adaption for these formulas, assume a source cloud with a concentration distribution that implies a given dosage at a point for this cloud; that is, the dosage per event. If there are a number of similar clouds, discretely spaced, then for each cloud we obtain a dosage for each cloud whose sum corresponds to the total dosage for the entire event.

In summary, the Multilayer Diffusion Model is composed of six submodels. Models 1 and 3 are designed to distinguish between the two sources of toxic cloud formation — the ground cloud during the initial launch phase (Model 3) and the plume cloud after the initial launch phase (Model 1). From the standpoint of environmental impact, the description of the fields of the ground deposition of materials from the ground cloud is of primary significance; this description is afforded by Model 3. Generally, this model is employed in the surface layer, but can be employed in any layer where the source does not extend through the entire layer.

Model 2 was designed to account for a lack of turbulent mixing which can occur in the upper atmosphere. Model 4 is employed when a change in meteorological condition occurs during the downstream transport of the cloud. In the event of rain, the precipitation scavenging of both gases and particles can be accounted for in Model 5. The fallout of particulate matter on the ground is the domain of Model 6. These six submodels form the basic set of equations which are available to treat the diffusion problem. To model a specific launch of a vehicle, it is necessary to blend these equations and adjust the model parameters to the specific meteorological conditions of the launch, to the specific terrain around the launch site, and to the specific vehicle being launched; thus the degree of complexity in the diffusion model.

RESULTS OF THE CALCULATIONS

The results of the model concentration computations and descriptions of the meteorological regimes at Kennedy Space Center and Vandenberg Air Force Base, for which the calculations were made, are as follows.

Peak ground-level and 10-min average concentration calculations were made for the nine meteorological regimes at KSC and the six meteorological regimes at VAFB as indicated in Table 2. As noted in the table, the first three regimes listed under KSC are "typical" regimes. Also in Table 2, ground-level concentrations were calculated for a meteorological regime in which a stationary front extended from east to west through central Florida in the vicinity of KSC on October 2, 1972. Ground-level concentrations were also calculated for three meteorological regimes associated with the approach and passage of a cold front at KSC during the period from October 19 to 21, 1972. Calculations were made for another case in which a cold front was located south of KSC on November 26, 1972. Finally, concentrations on November 27, 1972, were calculated for a regime where a fair-weather, high pressure regime existed over the Southeastern United States.

As presented in Table 2, concentration calculations were made at VAFB for three meteorological regimes in which the frontal activity influences dispersion. Calculations were made for October 10, 1972, (stationary upper-level trough west of VAFB), January 16, 1973, (cold front northwest of VAFB), and January 17, 1973, (cold front south of VAFB).

Concentration Calculations for Kennedy Space Center

Fall, Spring, and Sea-Breeze Meteorological Regimes. The meteorological data used in the concentration calculations for the fall, spring, and sea-breeze regimes at KSC were derived from the mean monthly wind speed, wind direction, and temperature profiles for KSC [22, 23]. These profiles have been used in previous hazard calculations for launches at KSC [23]. A study of the KSC climatology indicated that the average depth of the surface mixing layer in the fall season associated with the easterly winds required to transport the ground cloud inland is approximately 1000 m. During the spring, there are occasions when the surface mixing layer reaches a depth of 2000 m. The afternoon sea breeze, which is common to all seasons, has an average surface mixing layer of 300 m. The vertical profiles of wind speed, wind direction, and temperature for these three regimes are shown in Figures 3, 4, and 5. Table 3 gives the calculated HCl, CO, and Al_2O_3 peak concentrations downwind from the normal launch of a Space Shuttle vehicle for the three regimes at KSC. The slow decrease of ground-level concentrations with distance is evident for all three regimes at some distance between 1 and 10 km and reflects the gradual change in the vertical distribution of material from the initial Gaussian form to a rectangular form brought about by multiple reflection between the base and top of the surface layer. The highest concentration in these three cases was the fall regime. Outside the KSC industrial area of 10 km, HCl was less than 2.0 ppm, 3.5 for CO, and 4.2 mg/m^3 for Al_2O_3 as presented in Table 3. Table 4 gives the 10-min average concentration for HCl at KSC ranging from 1.39 to less than 0.01 ppm from 1 to 80 km for all nine meteorological conditions listed, which is well below the applicable limits developed by the NAS/NRC Committee on Toxicology [24, 25].

Pre-Cold Front, Cold Front, and Post-Cold Front Meteorological Regimes. Ground-level concentrations downwind from the launch pad were calculated for three meteorological regimes associated with the approach and passage of a cold front. The meteorological data of October 19, 20, and 21, 1972, were selected to be representative of these regimes at KSC. Figures 6, 7, and 8 show the vertical profiles of wind speed, wind direction, and temperature at 0700 Eastern Standard Time (EST) for the three days. At 0700 EST on October 19, a cold front was located northwest of Florida, extending from

Georgia through Southeast Alabama and then westward. Florida weather was fair with scattered high clouds and local haze conditions. The KSC 0700 EST sounding showed a stable layer from the surface to about 21[illegible] m above the ground. At 0700 EST on October 20, the cold front was oriented from east to west and was located just to the south of KSC. Rain and rain showers were occurring in the vicinity of the front. The KSC 0700 EST sounding indicates the presence of a moist, unstable air mass over KSC with a surface mixing layer extending to about 2000 m. The cold front had moved south into the Straits of Florida by 0700 EST on October 21. The 0700 EST sounding at KSC indicates a surface mixing layer depth of approximately 1400 m with dry, warm air aloft.

The calculated HCl peak ground-level concentrations as given in Table 3 at a downwind distance of 10 km are 0.7, 1.0, and 2.6 ppm for the pre-cold front, cold front, and post-cold front at KSC.

Additional Meteorological Regimes at KSC. Table 3 gives the peak concentration calculations for a stationary front south of KSC, a cold front south of KSC, and a fair-weather, high pressure regime at KSC for measurements at 10 km on October 2, 1972, November 26, 1972, and November 27, 1972.

Peak concentration calculations for HCl at the 10-km downwind distance were 1.2, 3.2, and 0.2 ppm, respectively, as presented in Table 3. Table 4 gives the 10-min average concentration for HCl at KSC ranging from 1.39 to 0.01 ppm or less for all the meteorological regimes from 1 to 80 km, which is well below the applicable exposure limits of 4 ppm developed by the NAS/NRC Committee on Toxicology.

Concentration Calculations for Vandenberg Air Force Base

Morning and Afternoon Fair-Weather Regimes. In the absence of frontal activity, the weather in the lower 2000 to 3000 m at VAFB is dominated by the land-sea-breeze regime. The marine (subsidence) inversion is present at VAFB over 90 percent of the time in the summer and approximately 50 percent of the time in the winter. With the Pacific high centered to the west and a thermal low common over the California interior, the prevailing gradient wind in all seasons is from the north or notheast. Cold air drainage from canyons in the vicinity of the launch areas contribute to the offshore winds at night and during the morning. Figure 9 shows typical morning profiles of wind speed, wind direction, and temperature during this type of fair-weather regime. At the time of the sounding, the westerly sea breeze is beginning to develop near the surface with northeasterly winds above. The surface mixing layer extends to the base of the inversion which is about 400 m above the ground.

During the day the layer of onshore flow deepens as the sea breeze becomes well established. Figure 10 shows typical wind speed, wind direction, and temperature profiles for an afternoon sea-breeze regime; the inversion base is about 225 m above the surface. Relatively high inversions are also observed at VAFB, often associated with an upper level trough to the west. Figure 11 shows typical wind and temperature profiles for an afternoon sea-breeze regime with an inversion base approximately 775 m above the surface.

The results of the peak concentration calculations for the morning low level meteorological regime at VAFB are presented in Table 3. In Table 3 the peak concentration profiles for the afternoon sea-breeze, low level meteorological regime are given. At 10 km, the morning inversion measured 1.70 ppm, and the afternoon inversion was 2.4 ppm. Also as given in Table 3 the sea-breeze, high level inversion meteorological regime measured approximately 6.5 ppm at 10 km.

Additional Meteorological Regimes at VAFB. Table 3 presents the peak concentration calculations for a stationary, upper level trough west of VAFB, a cold front northwest of VAFB, and a cold front south of VAFB. HCl concentrations at 10 km were about 1.5, 1.2, and 1.8 ppm.

Table 5 shows the 10-min average concentrations for HCl at VAFB, ranging from 1.75 to 0.01 ppm from 1 to 80 km for all the meteorological regimes. These values are well below the applicable exposure limits of 4 ppm developed by the NAS/NRC Committee on Toxicology.

Summary of Results

Table 3 lists the calculated peak ground-level concentrations for each of the three pollutants of interest at downwind distances of 1, 2, 5, and 10 km from the launch pad for normal launches of the Space Shuttle at Kennedy Space Center and Vandenberg Air Force Base. The pollutant concentrations at distances of 5 and 10 km are enclosed by solid lines to indicate that they should receive primary attention in assessing the potential environment hazard of the Space Shuttle emissions. The model concentrations made concern the vertical distributions of material in the stabilized cloud of exhaust products. Accurate measurements of this distribution are not available. Evidence from photographic data and very limited ground-level pollutant concentration measurements strongly indicates that only very small concentrations of exhaust products are found near ground-level after the cloud has stabilized. High concentrations of exhaust products exist in the immediate vicinity of the launch pad during the first minute or so after ignition as the result of the lateral deflection of hot

exhaust products which may extend outward from the pad to a maximum radial distance of about 1 km. However, most of the hot exhaust products then ascend and are incorporated into the main body of the stabilized ground cloud. In our model calculations the assumption is that the exhaust products in the stabilized cloud have a Gaussian distribution which is centered at the cloud stabilization height and extends to the ground. This assumption appears to result in larger ground-level concentrations near the launch pad after cloud stabilization than actually occur, which in turn leads to overestimates of downwind ground-level concentrations in the first few kilometers.

The calculated peak ground-level concentrations at a downwind distance of 10 km are appropriate for use in assessing the potential hazard to uncontrolled populations because, at both KSC and VAFB, this is the minimum distance from the launch pad area to the boundaries of uncontrolled population areas. Under this assumption, the calculated HCl peak ground-level concentrations in Table 3 at KSC for normal Space Shuttle launches range from 3.2 to 0.2 ppm, and the HCl peak ground-level concentrations at VAFB range from 6.5 to 1.2 ppm.

As shown in Tables 4 and 5, the 10-min average concentrations for HCl range from 1.39 to less than 0.01 ppm from 1 to 80 km at KSC. At VAFB these values range from 1.75 to 0.01 ppm which is well below the applicable exposure limits of 4 ppm developed by the NAS/NRC Committee on Toxicology.

The 10-min average concentrations for CO for all the meteorological conditions (Tables 4 and 5) at KSC were 2.45 to 0.01 ppm from downwind distances 1 to 80 km from the launch pad, and at VAFB the measurements were 3.08 ppm to 0.02 ppm. These measurements for Al_2O_3 were 3.03 mg/m^3 to 0.01 mg/m^3 for KSC, and 3.97 to 0.03 mg/m^3 for the same conditions at VAFB.

TABLE 1. FUEL PROPERTIES OF SPACE SHUTTLE ENGINES

Total Mass Flow Rate (g/sec)		
All Solid Engines	(W_S)	9.45126×10^6
Liquid Engines	(W_L)	1.53316×10^6
Fuel Heat Content (cal/g)		
Solid Engines	(H_S)	691
Liquid Engines	(H_L)	500
Fuel Composition (percent by weight)		
HCl	(FM)	20.7
CO	(FM)	28.0
Al_2O_3	(FM)	30.4

TABLE 2. METEOROLOGICAL REGIMES FOR WHICH CONCENTRATION CALCULATIONS WERE MADE

Location	Meteorological Regime	Date
KSC	Fall Spring Sea-Breeze	Typical Regimes
	Cold Front North of KSC	October 19, 1972
	Cold Front Near KSC	October 20, 1972
	Cold Front South of KSC	October 21, 1972
	Stationary Front South of KSC	October 2, 1972
	Cold Front South of KSC	November 26, 1972
	Fair Weather, High Pressure	November 27, 1972
VAFB	Morning Sea-Breeze with Low Level Inversion Sea-Breeze with High Level Inversion	Typical Regimes
	Stationary Upper-Level Trough West of VAFB	October 10, 1972
	Cold Front Northwest of VAFB	January 16, 1973
	Cold Front South of VAFB	January 17, 1973

TABLE 3. SUMMARY OF PEAK GROUND-LEVEL CONCENTRATIONS FOR NORMAL LAUNCHES OF THE SPACE SHUTTLE AT KSC AND VAFB UNDER VARIOUS METEOROLOGICAL CONDITIONS

Meteorological Regime	Pollutant	Centerline Ground-Level Concentration			
		Distance from Launch Pad (km)			
		1	2	5	10
a. Kennedy Space Center					
Fall	HCl (ppm)	7.5	5.0	4.4	2.0
	CO (ppm)	13.4	8.0	7.5	3.5
	Al_2O_3 (mg/m^3)	18.0	10.1	9.2	4.2
Spring	HCl (ppm)	4.6	2.4	2.0	1.6
	CO (ppm)	8.2	3.6	3.2	3.0
	Al_2O_3 (mg/m^3)	10.0	5.2	4.4	3.6
Sea Breeze	HCl (ppm)	14.0	7.0	1.6	0.4
	CO (ppm)	24.0	12.5	2.8	0.7
	Al_2O_3 (mg/m^3)	32.2	15.5	3.5	0.9
Cold Front North of KSC (Oct. 19, 1972)	HCl (ppm)	19.0	7.0	2.3	0.7
	CO (ppm)	33.0	12.5	4.0	1.3
	Al_2O_3 (mg/m^3)	42.0	16.0	5.1	1.7
Cold Front Near KSC (Oct. 20, 1972)	HCl (ppm)	50.1	20.0	4.0	1.0
	CO (ppm)	90.0	34.0	7.0	1.7
	Al_2O_3 (mg/m^3)	100.0	44.0	9.0	2.3
Cold Front South of KSC (Oct. 21, 1972)	HCl (ppm)	9.2	3.6	3.1	2.6
	CO (ppm)	15.0	6.2	5.0	4.6
	Al_2O_3 (mg/m^3)	24.0	8.0	7.0	6.0
Stationary Front South of KSC (Oct. 2, 1972)	HCl (ppm)	3.2	2.1	2.1	1.2
	CO (ppm)	5.5	3.7	3.9	2.1
	Al_2O_3 (mg/m^3)	7.0	4.5	5.0	2.7

TABLE 3. (Concluded)

Meteorological Regime	Pollutant	Centerline Ground-Level Concentration			
		Distance from Launch Pad (km)			
		1	2	5	10
Cold Front South of KSC (Nov. 26, 1972)	HCl (ppm)	10.1	4.2	3.5	3.2
	CO (ppm)	20.0	7.5	6.0	5.8
	Al_2O_3 (mg/m^3)	30.0	9.8	7.5	7.5
Fair Weather, High Pressure (Nov. 27, 1972)	HCl (ppm)	9.5	4.4	0.8	0.2
	CO (ppm)	16.0	7.5	1.5	0.4
	Al_2O_3 (mg/m^3)	20.0	10.0	2.0	0.5
b. Vandenberg Air Force Base					
Morning Inversion	HCl (ppm)	20.0	11.5	5.5	1.7
	CO (ppm)	34.0	19.7	9.5	3.0
	Al_2O_3 (mg/m^3)	45.0	24.0	12.0	3.8
Sea Breeze with Low Level Inversion	HCl (ppm)	21.1	11.2	4.7	2.4
	CO (ppm)	37.2	19.7	8.2	4.2
	Al_2O_3 (mg/m^3)	47.6	25.3	10.5	5.3
Sea Breeze with High Level Inversion	HCl (ppm)	17.3	11.7	10.5	6.5
	CO (ppm)	30.4	20.5	18.5	11.4
	Al_2O_3 (mg/m^3)	39.2	26.5	23.8	14.7
Stationary Upper Level Trough West of VAFB (Oct. 10, 1972)	HCl (ppm)	5.4	2.3	1.9	1.5
	CO (ppm)	9.5	4.1	3.5	2.7
	Al_2O_3 (mg/m^3)	12.0	5.4	4.4	3.5
Cold Front Northwest of VAFB (Jan. 16, 1973)	HCl (ppm)	17.0	7.0	3.6	1.2
	CO (ppm)	28.0	12.0	6.2	2.0
	Al_2O_3 (mg/m^3)	36.0	16.0	8.0	2.7
Cold Front South of VAFB (Jan. 17, 1973)	HCl (ppm)	7.0	2.6	1.8	1.8
	CO (ppm)	8.2	3.2	3.0	3.2
	Al_2O_3 (mg/m^3)	16.0	6.0	4.0	4.0

TABLE 4. SUMMARY OF 10-min AVERAGE CENTERLINE CONCENTRATIONS FOR SPACE SHUTTLE LAUNCHES AT KSC (POLLUTANT CONCENTRATIONS FOR HCl AND CO ARE IN ppm WHILE THOSE FOR Al_2O_3 ARE IN mg/m^3)

Meteorological Regime	Pollutant	Centerline Ground-Level Concentration						
		Distance from Launch Pad (km)						
		1	2	5	10	20	40	80
Fall	HCl	0.25	0.38	0.69	0.42	0.22	0.18	0.04
	CO	0.44	0.66	1.22	0.74	0.38	0.19	0.07
	Al_2O_3	0.54	0.82	1.51	0.92	0.48	0.23	0.09
Spring	HCl	0.10	0.10	0.25	0.29	0.18	0.09	0.04
	CO	0.16	0.14	0.42	0.52	0.33	0.16	0.80
	Al_2O_3	0.22	0.21	0.54	0.64	0.40	0.20	0.15
Sea Breeze	HCl	0.42	0.38	0.19	0.10	0.05	0.02	0.01
	CO	0.73	0.67	0.33	0.17	0.09	0.04	0.01
	Al_2O_3	0.92	0.84	0.42	0.22	0.11	0.05	0.02
Stationary Front South of KSC (10-2-72)	HCl	0.38	0.60	1.39	0.96	0.33	0.09	0.02
	CO	0.66	1.06	2.45	1.69	0.59	0.16	0.04
	Al_2O_3	0.82	1.72	3.03	2.10	0.73	0.20	0.05
Cold Front North of KSC (10-19-72)	HCl	0.39	0.30	0.20	0.10	0.05	0.02	0.01
	CO	0.68	0.53	0.34	0.18	0.09	0.04	0.02
	Al_2O_3	0.87	0.68	0.44	0.23	0.11	0.06	0.02
Cold Front Near KSC (10-20-72)	HCl	0.57	0.37	0.17	0.09	0.05	0.02	0.01
	CO	1.01	0.64	0.31	0.16	0.08	0.04	0.02
	Al_2O_3	1.26	0.81	0.38	0.20	0.10	0.05	0.03
Cold Front South of KSC (10-21-72)	HCl	0.17	0.15	0.37	0.51	0.32	0.16	0.06
	CO	0.88	0.87	0.80	0.94	0.57	0.29	0.11
	Al_2O_3	0.37	0.33	0.81	1.14	0.71	0.36	0.14
Cold Front South of KSC (11-26-72)	HCl	0.25	0.19	0.39	0.71	0.60	0.28	0.09
	CO	0.43	0.33	0.68	1.25	1.05	0.49	0.16
	Al_2O_3	0.55	0.42	0.86	1.59	1.34	0.63	0.20
Fair Weather High Pressure (11-27-72)	HCl	0.62	0.47	0.19	0.10	0.04	0.01	0.00
	CO	1.09	0.83	0.34	0.17	0.07	0.02	0.01
	Al_2O_3	1.46	1.10	0.46	0.22	0.10	0.03	0.01

TABLE 5. SUMMARY OF 10-min AVERAGE CENTERLINE CONCENTRATIONS FOR SPACE SHUTTLE LAUNCHES AT VAFB (POLLUTANT CONCENTRATIONS FOR HCl AND CO ARE IN ppm WHILE THOSE FOR Al_2O_3 ARE IN mg/m^3)

Meteorological Regime	Pollutant	Centerline Ground-Level Concentration						
		Distance from Launch Pad (km)						
		1	2	5	10	20	40	80
Morning	HCl	0.69	0.81	0.79	0.42	0.21	0.10	0.03
	CO	1.10	1.30	1.34	0.72	0.37	0.15	0.05
	Al_2O_3	1.43	1.69	1.74	0.94	0.48	0.20	0.06
Sea Breeze with Low Level Inversion	HCl	0.63	0.46	0.20	0.10	0.05	0.07	0.01
	CO	1.11	0.81	0.35	0.18	0.08	0.05	0.02
	Al_2O_3	1.42	1.04	0.45	0.23	0.12	0.07	0.03
Sea Breeze with High Level Inversion	HCl	0.63	0.85	1.75	1.18	0.61	0.31	0.16
	CO	1.11	1.50	3.08	2.07	1.08	0.55	0.28
	Al_2O_3	1.43	1.93	3.97	2.67	1.39	0.71	0.36
Stationary Upper Level Trough (10/10/73)	HCl	0.13	0.12	0.29	0.34	0.16	0.07	0.02
	CO	0.23	0.21	0.50	0.60	0.29	0.12	0.04
	Al_2O_3	0.29	0.27	0.64	0.76	0.36	0.15	0.05
Cold Front Northwest of VAFB (1/16/73)	HCl	0.28	0.25	0.30	0.18	0.10	0.05	0.02
	CO	0.50	0.44	0.52	0.31	0.17	0.08	0.03
	Al_2O_3	0.64	0.57	0.68	0.41	0.22	0.11	0.04
Cold Front South of VAFB (1/17/73)	HCl	0.19	0.14	0.24	0.46	0.44	0.21	0.06
	CO	0.22	0.18	0.41	0.84	0.80	0.37	0.11
	Al_2O_3	0.44	0.32	0.54	1.07	1.01	0.47	0.15

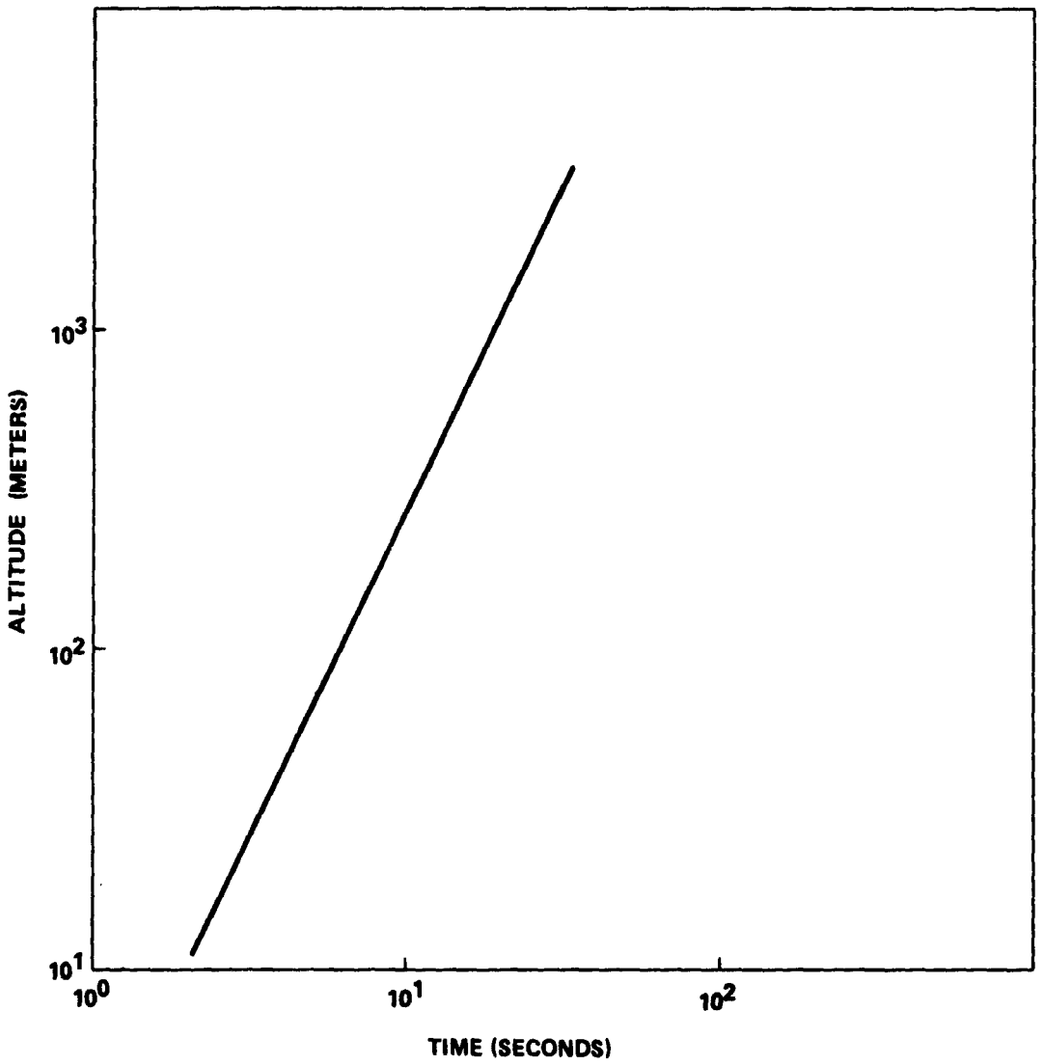

Figure 1. Height of the Space Shuttle vehicle as a function of time (t_R) after ignition.

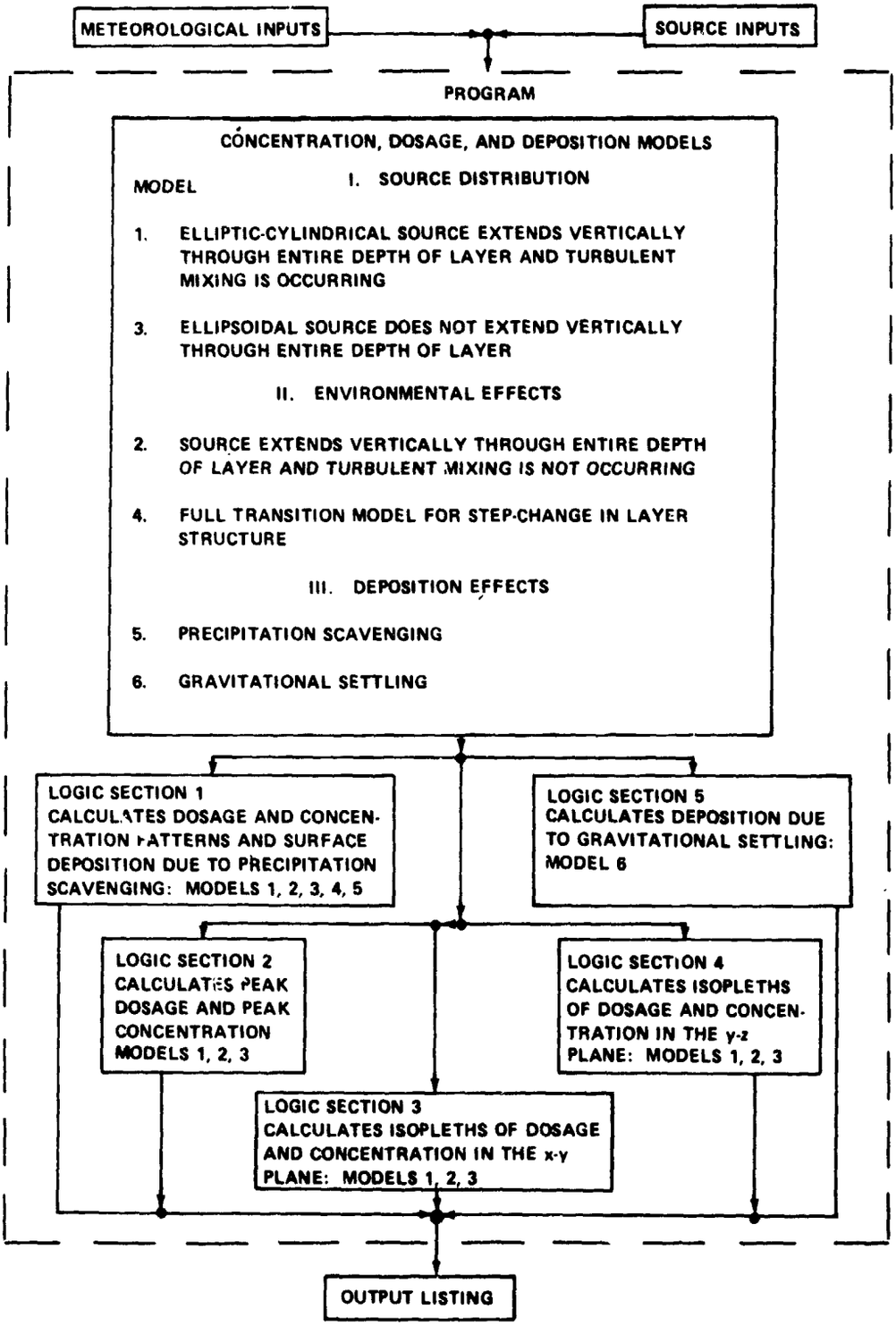

Figure 2. Block diagram of the computer program for the NASA/MSFC Multilayer Diffusion Model.

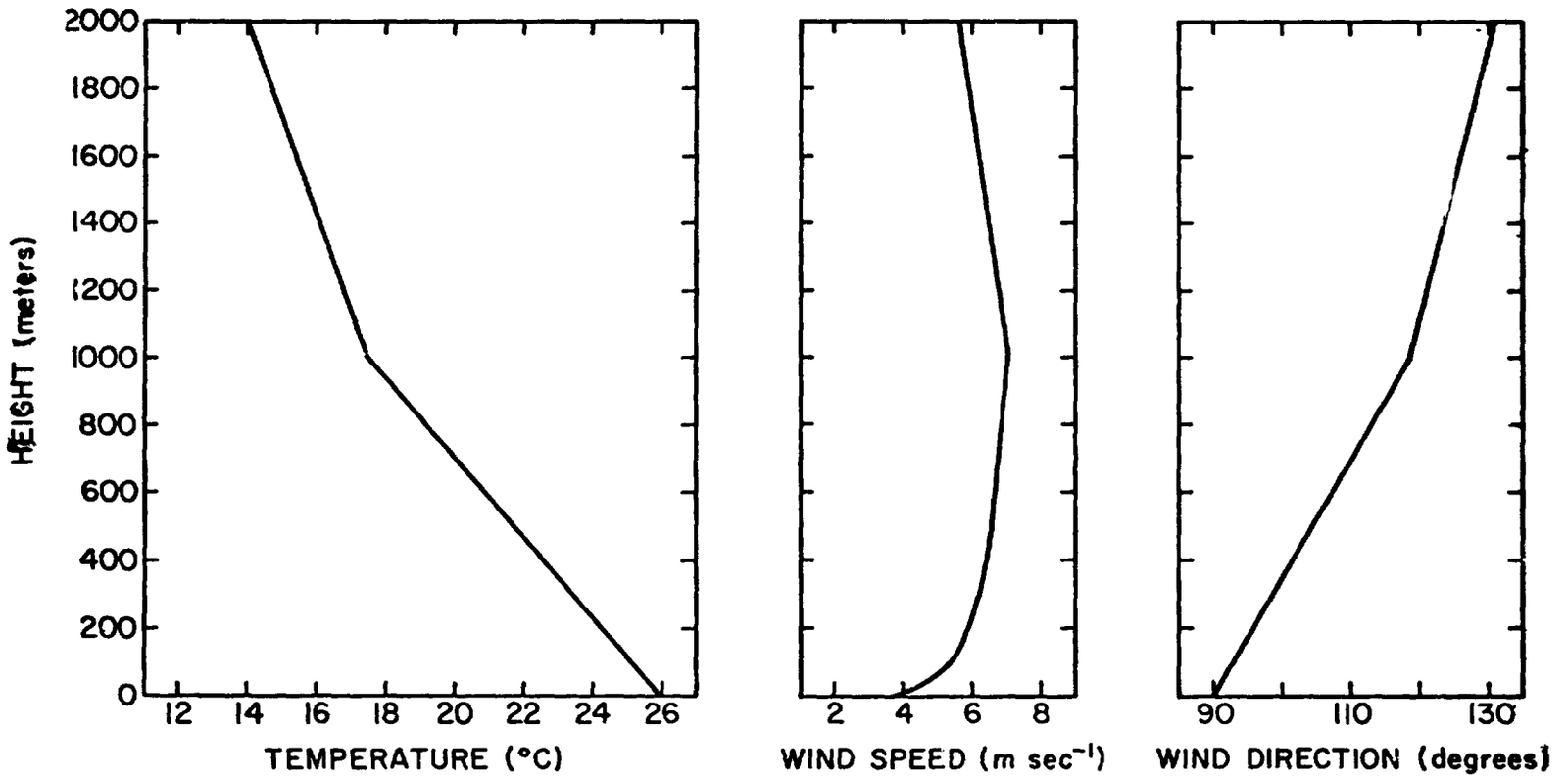

Figure 3. Vertical profiles of temperature, wind speed, and wind direction for the fall meteorological regime at KSC.

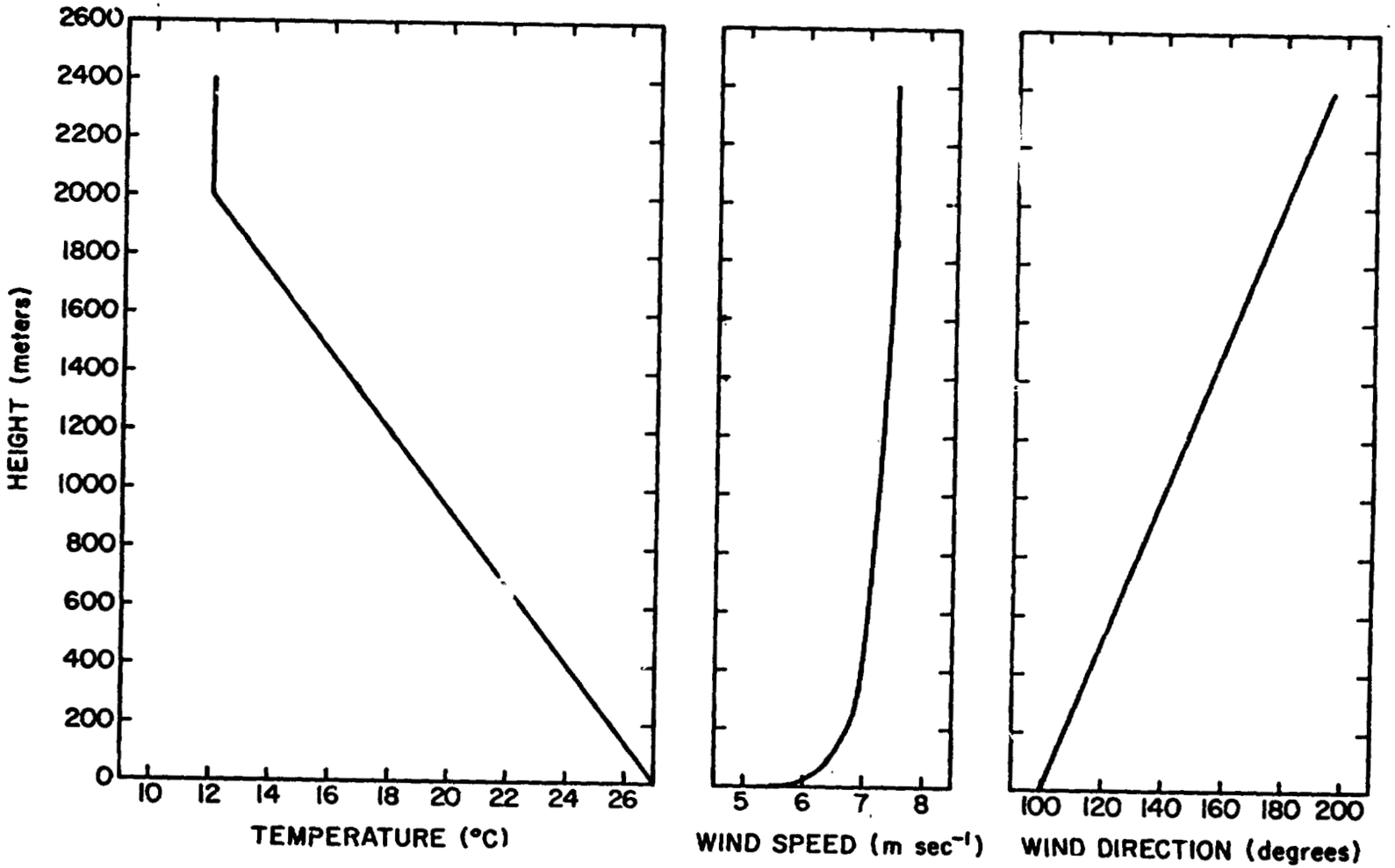

Figure 4. Vertical profiles of temperature, wind speed, and wind direction for the spring meteorological regime at KSC.

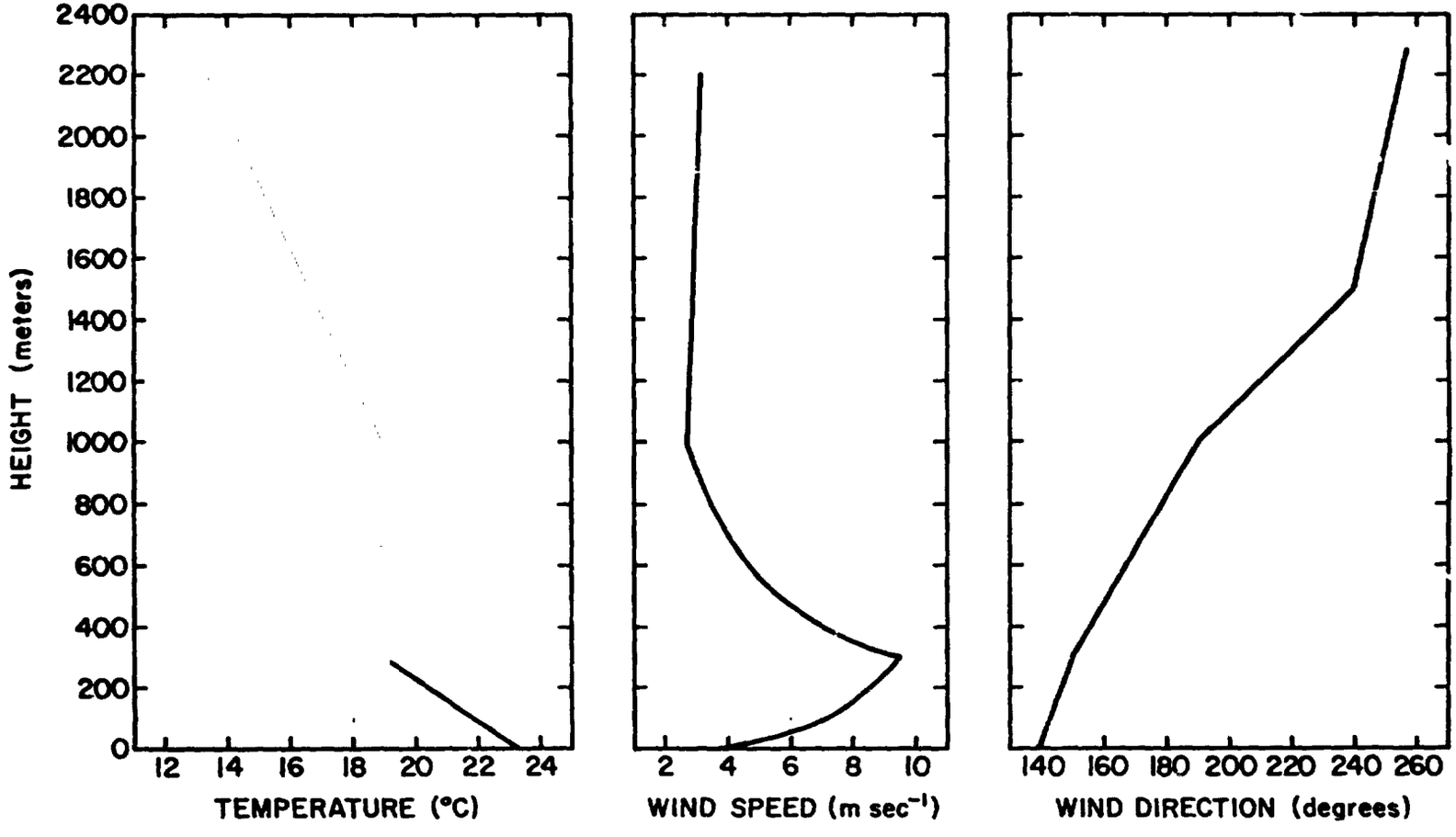

Figure 5. Vertical profiles of temperature, wind speed, and wind direction for the sea-breeze meteorological regime at KSC.

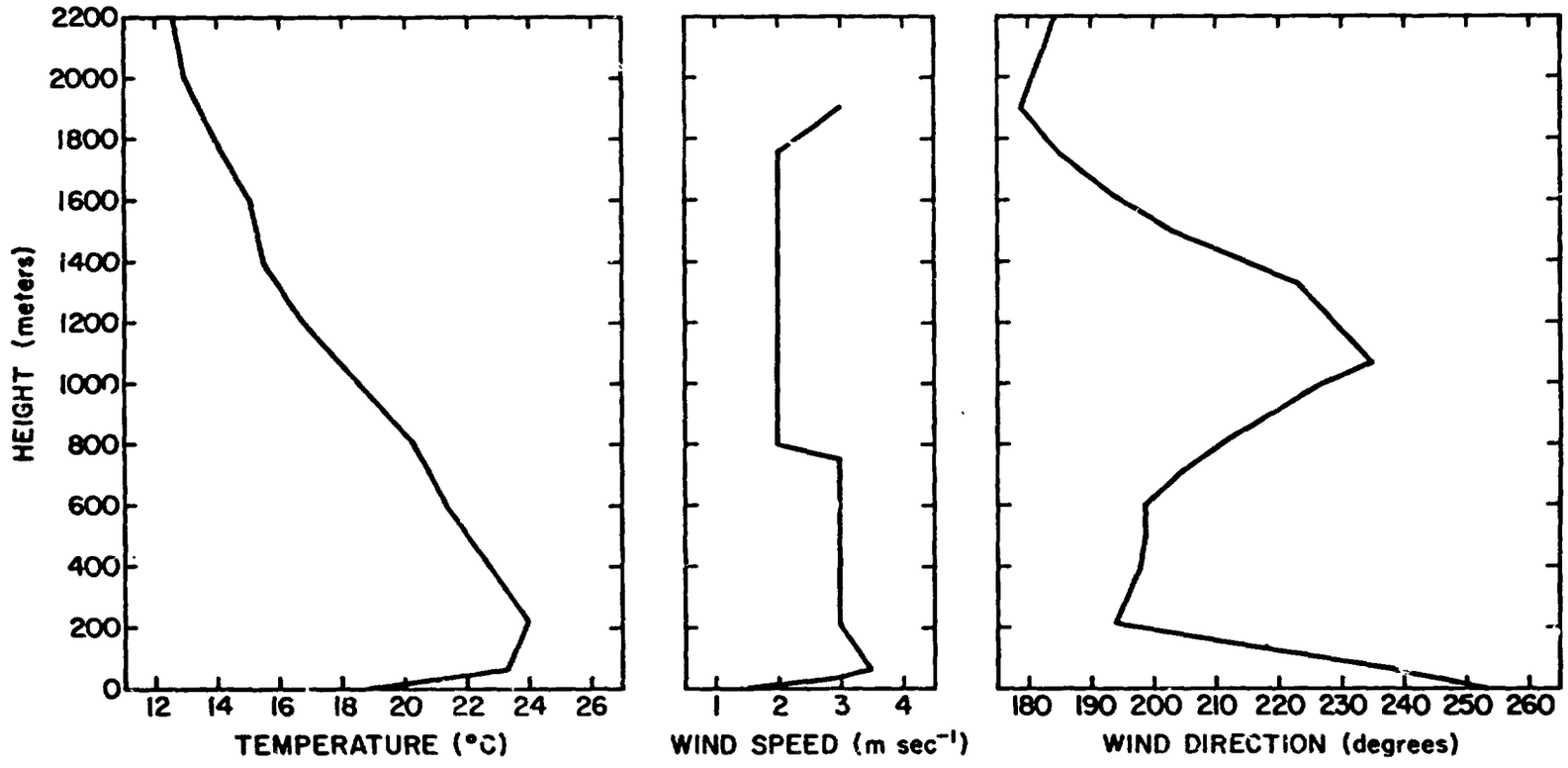

Figure 6. Vertical profiles of temperature, wind speed, and wind direction for the fair-weather, pre-cold front meteorological regime at KSC (October 19, 1972).

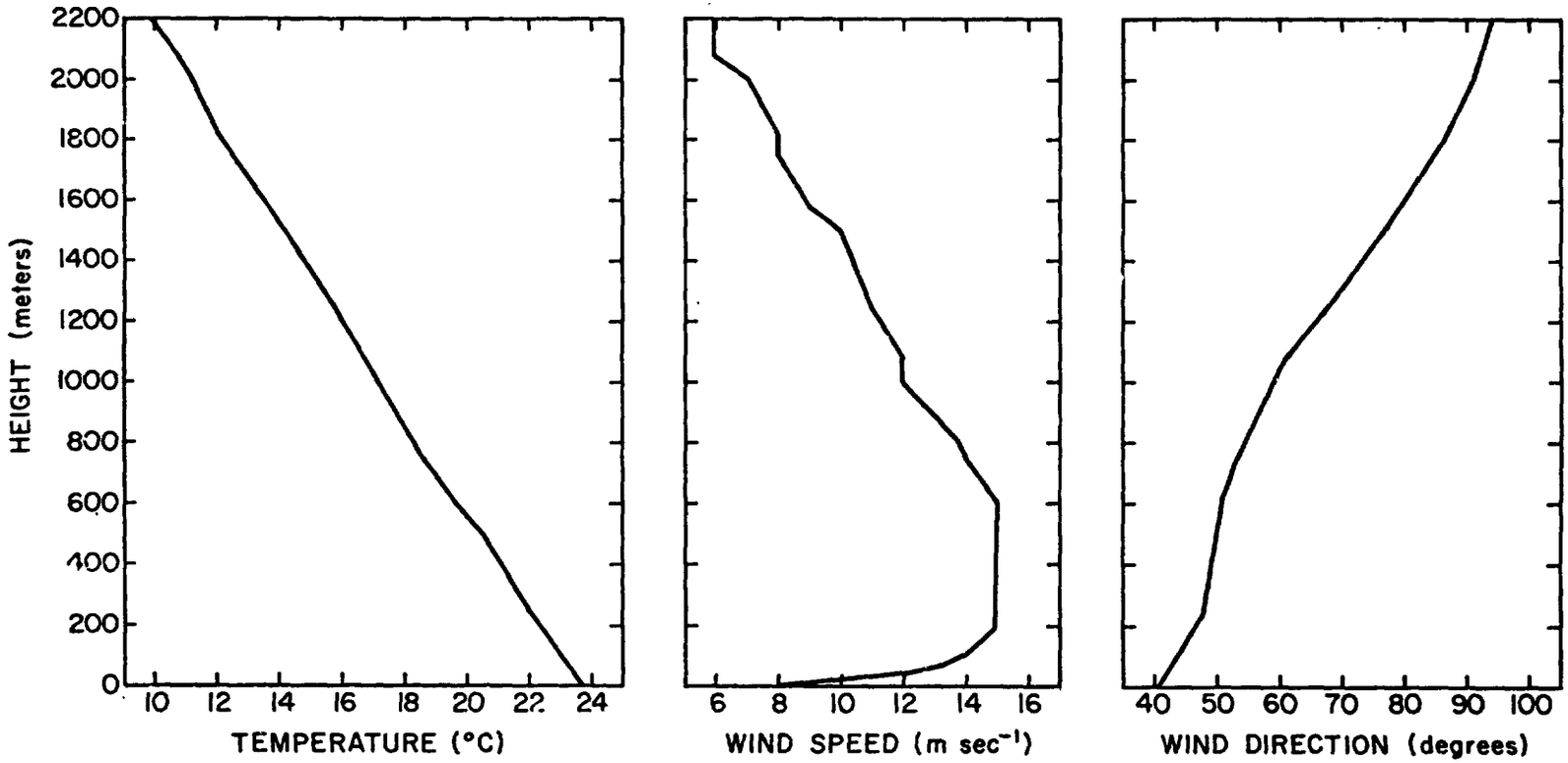

Figure 7. Vertical profiles of temperature, wind speed, and wind direction for the cold front meteorological regime at KSC (October 20, 1972).

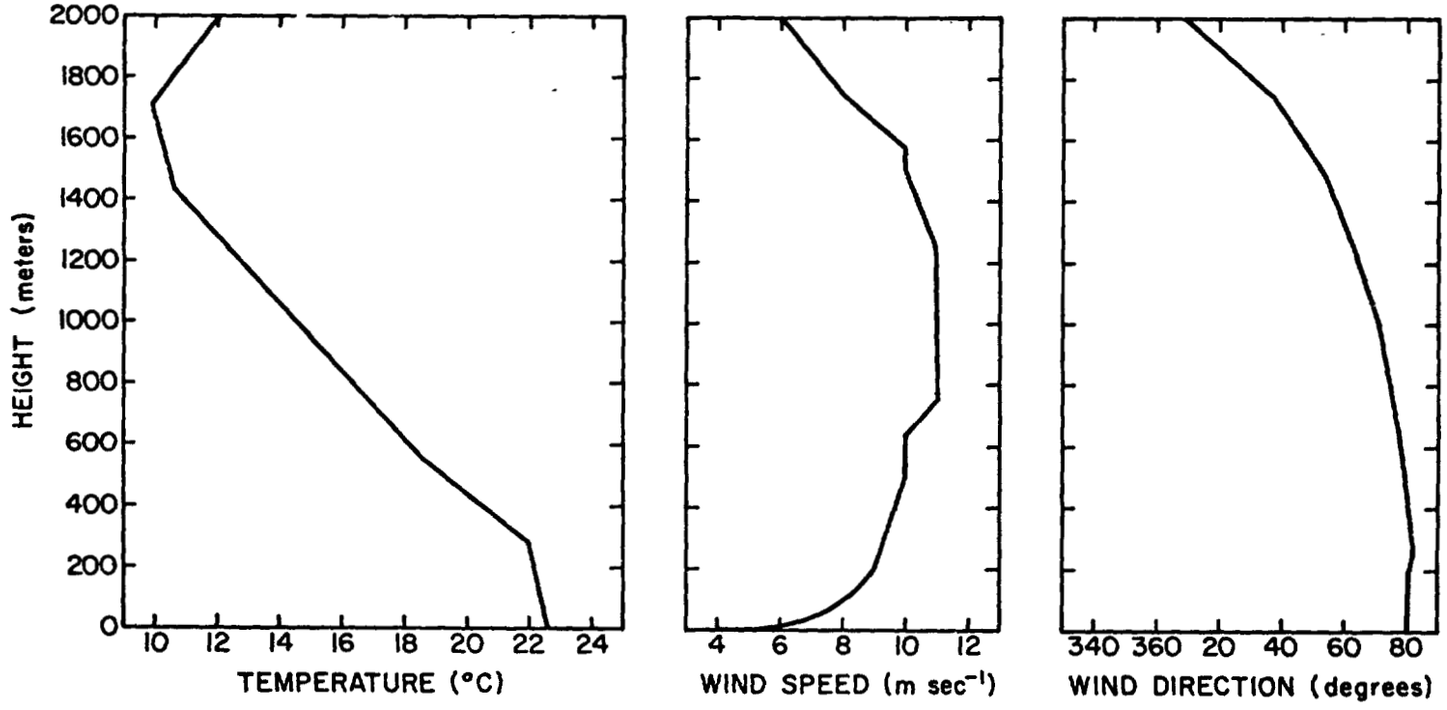

Figure 8. Vertical profiles of temperature, wind speed, and wind direction for the post-cold front meteorological regime at KSC (October 21, 1972).

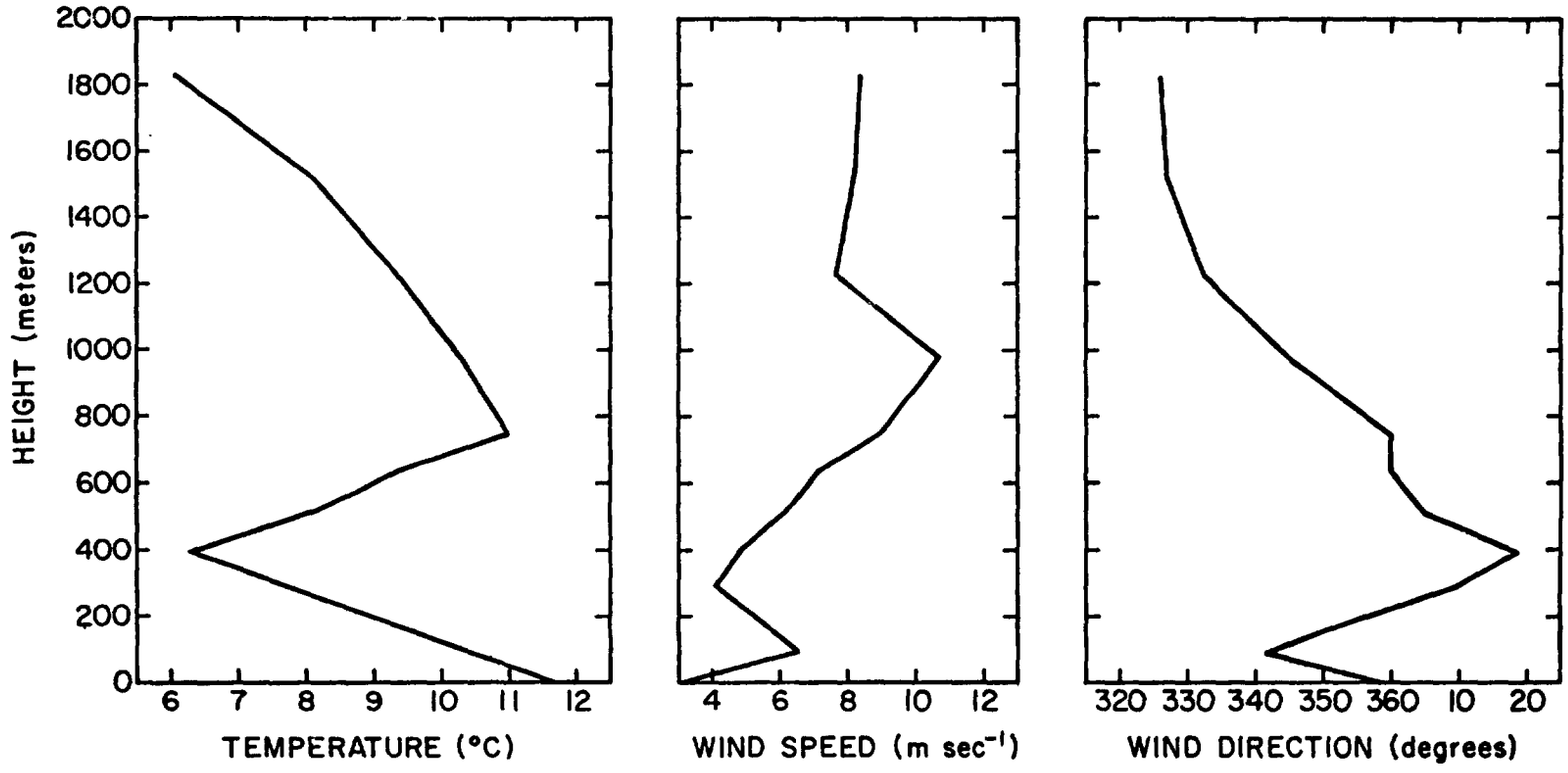

Figure 9. Vertical profiles of temperature, wind speed, and wind direction for the morning low level inversion meteorological regime at VAFB.

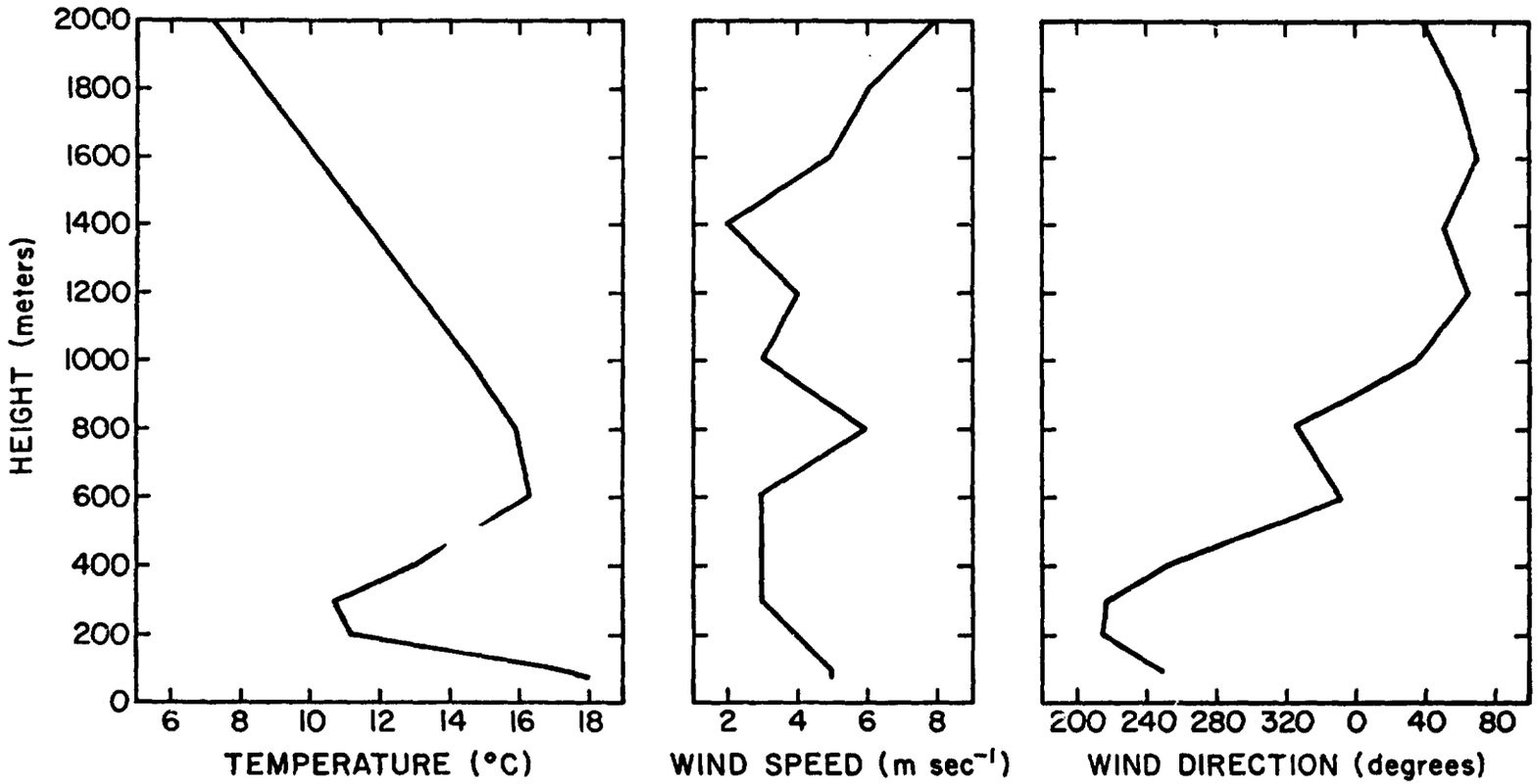

Figure 10. Vertical profiles of temperature, wind speed, and wind direction for the afternoon sea-breeze, low level inversion meteorological regime at VAFB.

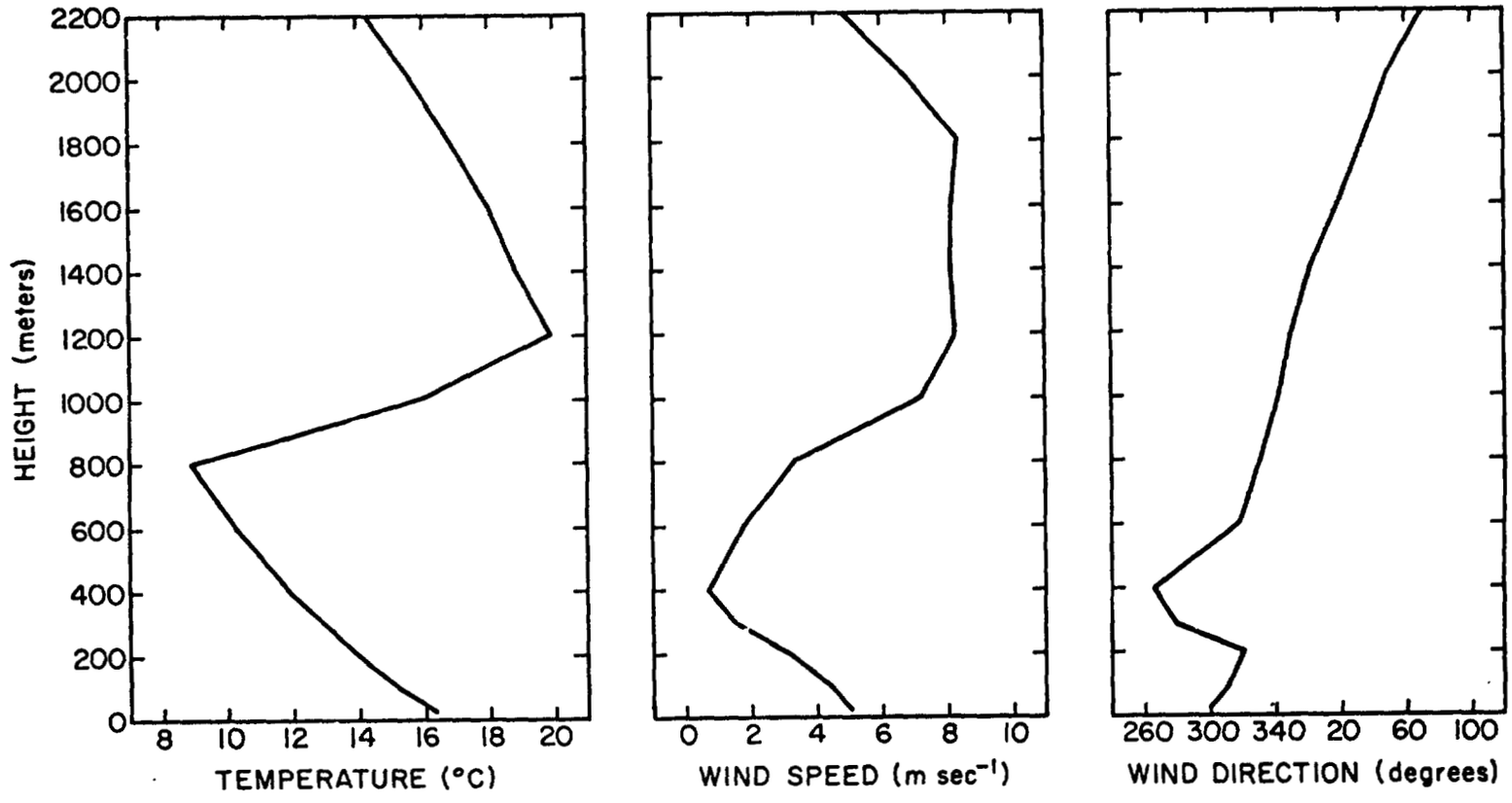

Figure 11. Vertical profiles of temperature, wind speed, and wind direction for the afternoon sea-breeze, high level inversion meteorological regime at VAFB.

APPENDIX A

CLOUD RISE FORMULAE [1]

In order to determine whether an adiabatic or stable cloud rise relation should be utilized, it is necessary to determine the vertical potential temperature gradient ($\partial\theta/\partial z$) which is described by

$$\frac{\partial\theta}{\partial z} = \frac{\theta}{T}\frac{\partial T}{\partial z} + \frac{g}{c_p} \approx \frac{\partial T}{\partial z} + \frac{g}{c_p} \qquad \text{(A-1)}$$

and g/c_p is equal to the adiabatic lapse rate (10° C/km).

In addition, θ and T are the potential and ambient temperature, g is the gravitational acceleration, and c_p is the specific heat of air. If

$$\frac{\partial\theta}{\partial z} \leqq 0 \quad , \qquad \text{(A-2)}$$

the adiabatic cloud rise relation is used.

The maximum cloud rise z_{mI} downwind from an instantaneous source in adiabatic atmosphere is given by

$$z_{mI} = \left[\frac{2F_I t_{sI}^2}{\gamma_I^3} + \left(\frac{r_R}{\gamma_I}\right)^4\right]^{1/4} - \frac{r_R}{\gamma_I} \quad , \qquad \text{(A-3)}$$

whereas, the maximum cloud rise z_{mI} downwind from an instantaneous source in a stable atmosphere is given by

$$z_{mI} = \left[\frac{8F_I}{\gamma_I^3 s} + \left(\frac{r_R}{\gamma_I}\right)^4\right]^{1/4} - \frac{r_R}{\gamma_I} \quad , \qquad \text{(A-4)}$$

where F_I is the instantaneous buoyancy parameter $(3gQ_I/4\pi\rho c_p T)$, Q_I is the effective heat released, ρ is the density of ambient air, γ_I is the entrainment coefficient, r_R is the initial cloud radius at the surface, s accounts for the vertical gradient of the potential temperature, and t_{sI} is the time to reach stabilization. The subscript I means instantaneous and is used to flag a difference in the cloud rise models. The buoyancy terms, which are a function of the heat released and the type of entrainment, spherical and cylindrical, reflect the major difference in the two sources.

Equations (A-3) and (A-4) assume that the initial upward momentum imparted to the exhaust gases by reflection from the ground surface and launch pad hardware is insignificant in comparison with the thermal buoyancy flux. These relations are normally used with solid rocket motors.

The following formulae for the maximum buoyant rise of clouds from continuous sources are also based on procedures similar to those given by Briggs (1970). The maximum cloud rise z_{mc} downwind from a continuous source in an adiabatic atmosphere is given by

$$z_{mc} = \left[\frac{3F_c x_{sc}^2}{2\gamma_c^2 \bar{u}^3} + \left(\frac{r_R}{\gamma_c} \right)^3 \right]^{1/3} - \frac{r_R}{\gamma_c} \quad . \tag{A-5}$$

The maximum cloud rise z_{mc} downwind from a continuous source in a stable atmosphere is given by

$$z_{mc} = \left[\frac{6F_c}{\bar{u}\gamma_c^2 s} + \left(\frac{r_R}{\gamma_c} \right)^3 \right]^{1/3} - \frac{r_R}{\gamma_c} \quad , \tag{A-6}$$

where F_c is the continuous buoyancy flux parameter and is equal to $gQ_c/\pi\rho c_p T$. The subscript c implies that the associated parameter is unique to the continuous source. The primary difference in these continuous source relations is that the temperature constraint in the stable atmosphere results in a buoyancy damping.

Equations (A-5) and (A-6) assume that the initial momentum flux inparted to the cloud by dynamic forces is negligible in comparison to buoyancy flux. Again, experience in calculating cloud rise for normal launches of large liquid fueled rockets and for static firings has shown that this assumption is reasonable.

APPENDIX B

CONCENTRATION-DOSAGE FORMULATION FOR NASA/MSFC MULTILAYER DIFFUSION MODEL

The fundamental relation for the concentration-dosage calculation will be presented for the ellipsoidal source used in Model 3. These relations are appropriate to the elliptic-cylindrical distribution of Model 1 if the vertical dispersive interaction is neglected. This part of the appendix is complex; therefore, its use is recommended only when a detailed scientific knowledge is required.

The dosage equation for Model 3 in the Kth layer is given by the expression

$$
\begin{aligned}
D_K\left\{x_K, y_K, z_{BK} < z_K < z_{TK}\right\} = \frac{Q_K}{2\pi\sigma_{yK}\sigma_{zK}\bar{u}_K} \Bigg\{ & \left\{\exp\left[\frac{-y_K^2}{2\sigma_{yK}^2}\right]\right\}\left\{\exp\left[\frac{-(H_K - z_K)^2}{2\sigma_{zK}^2}\right]\right. \\
& + \exp\left[\frac{-(H_K - 2z_{BK} + z_K)^2}{2\sigma_{zK}^2}\right] \\
& + \sum_{i=1}^{\infty} \Bigg\{ \exp\left[\frac{-\left(2i(z_{TK} - z_{BK}) - (H_K - 2z_{BK} + z_K)\right)^2}{2\sigma_{zK}^2}\right] \\
& + \exp\left[\frac{-\left(2i(z_{TK} - z_{BK}) + (H_K - z_K)\right)^2}{2\sigma_{zK}^2}\right] \\
& + \exp\left[\frac{-\left(2i(z_{TK} - z_{BK}) - (H_K - z_K)\right)^2}{2\sigma_{zK}^2}\right] \\
& \left. + \exp\left[\frac{-\left(2i(z_{TK} - z_{BK}) + (H_K - 2z_{BK} + z_K)\right)^2}{2\sigma_{zK}^2}\right]\right\}\Bigg\} ,
\end{aligned}
\tag{B-1}
$$

where Q_K corresponds to the source strength or total mass of material in the layer and H_K is the height of the centroid of the stabilized cloud.

The standard deviation of the vertical dosage distribution (σ_{zK}) is defined by the expression

$$\sigma_{zK} = \sigma'_{EK} x_{rzK} \left(\frac{x_K + x_{zK} - x_{rzK}(1 - \beta_K)}{\beta_K x_{rzK}} \right)^{\beta_K} , \qquad \text{(B-2)}$$

where σ'_{EK} describes the mean standard deviation of the wind elevation angle, x_{zK} gives the vertical virtual distance, β_K accounts for vertical diffusion, and x_{rzK} is the distance over which rectilinear vertical expansion occurs downwind from an ideal point source in the Kth layer.

In the surface layer $(K = 1)$, the standard deviation of the wind elevation angle (σ_{ER}) at the height z_R is described by

$$\sigma_{EK}\{K = 1\} = \frac{\sigma_{ER}\left[(z_{TK}\{K = 1\})^{q+1} - (z_R)^{q+1}\right]}{(q + 1)(z_{TK}\{K = 1\} - z_R)(z_R)^q} \left(\frac{\pi}{180}\right) , \qquad \text{(B-3)}$$

where the power-law exponent (q) for the vertical profile of the standard deviation of the wind elevation angle in the surface layer is

$$q = \log\left(\frac{\sigma_{ETK}\{K = 1\}}{\sigma_{ER}}\right) \Big/ \log\left(\frac{z_{TK}\{K = 1\}}{z_R}\right) , \qquad \text{(B-4)}$$

where $\sigma_{ETK}\{K = 1\}$ is the standard deviation of the wind elevation angle at the top of the surface layer. Above the surface layer $(K > 1)$, the standard deviation of the wind elevation angle is

$$\sigma'_{EK}\{K > 1\} = (\sigma_{ETK} + \sigma_{EBK})\left(\frac{\pi}{360}\right) \quad , \tag{B-5}$$

where σ_{ETK} and σ_{EBK} are the standard deviations of the wind elevation angle at the top and the base of the layer.

The vertical virtual distance x_{zK} is given by the expression

$$\left\{\begin{array}{ll} \dfrac{\sigma_{zo}\{K\}}{\sigma'_{EK}} - x_{RzK} & ; \ \sigma_{zp}\{K\} \le \sigma'_{EK}\, x_{rzK} \\ \beta_K\, x_{rzK}\left(\dfrac{\sigma_{zo}\{K\}}{\sigma'_{EK}\, x_{rzK}}\right)^{1/\beta_K} - x_{RzK} + x_{rzK}(1 - \beta_K) & ; \ \sigma_{zo}\{K\} \ge \sigma'_{EK}\, x_{rzK} \end{array}\right\} , \tag{B-6}$$

where $\sigma_{zo}\{K\}$ is the standard deviation of the vertical dosage distribution at x_{RzK}, the distance from the source where the measurement is made in the Kth layer.

The remaining terms are common also to Model 1; that is, what has just been discussed is to account for the vertical expansion of the source cloud.

The quantity $\bar{u}_K$ in equation (B-1) is the mean cloud transport speed in the Kth layer. In the surface layer $(K = 1)$, the wind speed-height profile is defined according to the power-law expression

$$\bar{u}\{z_K, K = 1\} = \bar{u}_R\left(\frac{z_K\{K = 1\}}{z_R}\right)^p \quad , \tag{B-7}$$

where $\bar{u}_R$ is the mean wind speed measured at the reference height z_R and the power-law exponent (p) for the wind speed profile in the surface layer is described by

$$p = \log\left(\frac{\bar{u}_{TK}\{K=1\}}{\bar{u}_R}\right) \Big/ \log\left(\frac{z_{TK}\{K=1\}}{z_R}\right) \quad . \tag{B-8}$$

Here, $\bar{u}_{TK}\{K=1\}$ corresponds to the mean wind speed at the top of the surface layer $(z_{TK}\{K=1\})$. Thus, in the surface layer, the mean cloud transport speed $(u\{K=1\})$ is

$$\bar{u}_K\{K=1\} = \frac{\bar{u}_R}{(z_{TK}\{K=1\} - z_R)\, z_R^{\,p}} \int_{z_R}^{z_{TK}} (z_K\{K=1\})^p \, dz \quad , \tag{B-9}$$

which reduces to

$$\bar{u}_K\{K=1\} = \frac{\bar{u}_R \left[(z_{TK}\{K=1\})^{1+p} - (z_R)^{1+p}\right]}{(z_{TK}\{K=1\} - z_R)(z_R)^p\,(1+p)} \quad . \tag{B-10}$$

In layers above the surface layer $(K > 1)$, the wind speed-height profile $(\bar{u}\{z_K, K > 1\})$ is assumed linear and is defined as

$$\bar{u}\{z_K, K > 1\} = \bar{u}_{BK} + \left(\frac{\bar{u}_{TK} - \bar{u}_{BK}}{z_{TK} - z_{BK}}\right)(z_K - z_{BK}) \quad , \tag{B-11}$$

where $\bar{u}_{TK}$ and $\bar{u}_{BK}$ describe the mean wind speed at the top of the layer and at the base of the layer, respectively. In the Kth layer $(K > 1)$, the mean cloud transport speed $(u_K\{K > 1\})$ is

$$\bar{u}_K\{K > 1\} = (\bar{u}_{TK} + \bar{u}_{BK})/2 \quad . \tag{B-12}$$

The standard deviation of the crosswind dosage distribution (σ_{yK}) is defined by

$$\sigma_{yK} = \left\{ \left[\sigma'_{AK}\{\tau_K\} \, x_{ryK} \left(\frac{x_K + x_{yK} - x_{ryK}(1 - \alpha_K)}{\alpha_K \, x_{ryK}} \right)^{\alpha_K} \right]^2 + \left[\frac{\Delta\theta'_K \, x_K}{4.3} \right]^2 \right\}^{1/2} , \qquad \text{(B-13)}$$

where $\sigma'_{AK}\{\tau_K\}$ corresponds to the mean layer standard deviation of the wind azimuth for the cloud stabilization time (τ_K). In the surface layer $(K = 1)$,

$$\sigma'_{AK}\{\tau_K, K = 1\} = \frac{\sigma'_{AR}\{\tau_K\} \left[(z_{TK}\{K = 1\})^{m+1} - (z_R)^{m+1} \right]}{(m + 1)(z_{TK}\{K = 1\} - z_R)(z_R)^m} , \qquad \text{(B-14)}$$

where the standard deviation of the wind azimuth angle $(\sigma'_{AR}\{\tau_K\})$ at height z_R and for the cloud stabilization time τ_K is

$$\sigma'_{AR}\{\tau_K\} = \sigma_{AR}\{\tau_{oK}\} \left(\frac{\tau_K}{\tau_{oK}} \right)^{1/5} \left(\frac{\pi}{180} \right) . \qquad \text{(B-15)}$$

Here $\sigma_{AR}\{\tau_{oK}\}$ is the standard deviation of the wind azimuth angle at height z_R and for the reference time period (τ_{oK}), and the power-law exponent (m) for the vertical profile of the standard deviation of the wind azimuth angle in the surface layer is

$$m = \log \left(\frac{\sigma'_{ATK}\{\tau_K, K = 1\}}{\sigma'_{AR}\{\tau_K\}} \right) \Big/ \log \left(\frac{z_{TK}\{K = 1\}}{z_R} \right) . \qquad \text{(B-16)}$$

Then,

$$\sigma'_{ATK}\{\tau_K,\ K=1\} = \sigma_{ATK}\{\tau_{oK},\ K=1\}\left(\frac{\tau_K}{\tau_{oK}}\right)^{1/5}\left(\frac{\pi}{180}\right) \quad , \quad \text{(B-17)}$$

where $\sigma_{ATK}\{\tau_{oK},\ K=1\}$ is the standard deviation of the wind azimuth angle at the top of the surface layer for the reference time period. For layers above the surface $(K > 1)$,

$$\sigma'_{ATK}\{\tau_K,\ K>1\} = \left(\sigma'_{ATK}\{\tau_K\} + \sigma'_{ABK}\{\tau_K\}\right)\Big/2 \quad , \quad \text{(B-18)}$$

where,

$$\sigma'_{ATK}\{\tau_K\} = \sigma_{ATK}\{\tau_{oK}\}\left(\frac{\tau_K}{\tau_{oK}}\right)^{1/5}\left(\frac{\pi}{180}\right) \quad \text{(B-19)}$$

Here $\sigma_{ATK}\{\tau_{oK}\}$ is the standard deviation of the wind azimuth angle at the top of the layer.

$$\sigma'_{ABK}\{\tau_K\} = \sigma_{ABK}\{\tau_{oK}\}\left(\frac{\tau_K}{\tau_{oK}}\right)^{1/5}\left(\frac{\pi}{180}\right) \quad , \quad \text{(B-20)}$$

where $\sigma_{ABK}\{\tau_{oK}\}$ is the standard deviation of the wind azimuth angle in degrees at the base of the layer for the reference time period (τ_{oK}).

The crosswind virtual distance is

$$x_{yK} = \frac{\sigma_{yo}\{K\}}{\sigma'_{AK}\{\tau_K\}} - x_{RyK} \qquad \text{(B-21)}$$

when

$$\sigma_{yo}\{K\} \leq \sigma'_{AK}\{\tau_K\}\, x_{ryK} \quad ,$$

or

$$x_{yK} = \alpha_K\, x_{ryK} \left(\frac{\sigma_{yo}\{K\}}{\sigma'_{AK}\{\tau_K\}\, x_{ryK}} \right)^{1/\alpha_K} - x_{RyK} + x_{ryK}(1 - \alpha_K) \qquad \text{(B-22)}$$

when

$$\sigma_{yo}\{K\} \geq \sigma'_{AK}\{\tau_K\}\, x_{ryK} \quad .$$

Here, $\sigma_{yo}\{K\}$ is the standard deviation of the lateral source dimension in the layer at downwind distance x_{RyK}, x_{ryK} is the distance over which rectilinear crosswind expansion occurs downwind from an ideal point source, and α_K describes the lateral diffusion in the layer. The vertical wind direction shear $(\Delta\theta'_K)$ in the layer is

$$\Delta\theta'_K = (\theta_{TK} - \theta_{BK}) \left(\frac{\pi}{180} \right) \quad , \qquad \text{(B-23)}$$

where θ_{TK} and θ_{BK} are the mean wind direction at the top and at the base of the layer, respectively.

The concentration algorithm is of the same form for the first three models; however, the dosage term (D_K) does depend on which model has been utilized, and thus adjusts the concentration description to the specific model of interest.

The maximum concentration for the first three models in the Kth layer is given by the expression

$$\chi_K\{x_K, y_K, z_K\} = \frac{D_K \bar{u}_K}{\sqrt{2\pi}\,\sigma_{xK}} \quad , \tag{B-24}$$

where the standard deviation of the alongwind concentration distribution (σ_{xK}) in the layer is

$$\sigma_{xK} = \left[\left(\frac{L\{x_K\}}{4.3}\right)^2 + \sigma_{xo}^{\,2}\{K\}\right]^{1/2} \tag{B-25}$$

and the alongwind cloud length $(L\{x_K\})$ for a point source in the layer at the distance x_K from the source is

$$L\{x_K\} = \begin{cases} \dfrac{0.28\,(\Delta\bar{u}_K)(x_K)}{\bar{u}_K} & ; \quad \Delta\bar{u}_K \geq 0 \\ 0 & ; \quad \Delta\bar{u}_K \leq 0 \end{cases} \quad , \tag{B-26}$$

where $\Delta\bar{u}_K$ is the vertical wind speed shear in the layer and is defined as

$$\Delta\bar{u}_K\{K=1\} = \bar{u}_{TK}\{K=1\} - \bar{u}_R \tag{B-27}$$

or

$$\Delta \bar{u}_K\{K > 1\} = \bar{u}_{TK} - \bar{u}_{BK} \quad , \tag{B-28}$$

and $\sigma_{xo}\{K\}$ is the standard deviation of the alongwind source dimension in the layer at the point of cloud stabilization. The above equation for $L\{x_K\}$ is based on the theoretical and empirical results reported by Tyldesley and Wallington [26] who analyzed ground-level concentration measurements made at a distance of 5 to 120 km downwind from instantaneous line-source releases.

The maximum centerline concentration for the model in the Kth layer is given by the expression

$$\chi_{CK}\{x_K, y_K = 0, z_K\} = \chi_K \Big/ \{\text{LATERAL TERM}\} \quad . \tag{B-29}$$

The average alongwind concentration is defined as

$$\bar{\chi}_K = D_K \Big/ t_{pK} \quad , \tag{B-30}$$

where the ground cloud passage time in seconds is

$$t_{pK} \cong 4.3\, \sigma_{xK} \Big/ \bar{u}_K \quad . \tag{B-31}$$

The time mean alongwind concentration in the Kth layer is defined by the expression

$$\chi_K\{x_K, y_K, z_K \; ; \; T_A\} = \frac{D_K}{T_A} \left\{ \operatorname{erf} \left(\frac{\bar{u}_K \, T_A}{2\sqrt{2}\, \sigma_{xK}} \right) \right\} \quad , \tag{B-32}$$

where T_A is the time in seconds over which concentration is to be averaged. The time mean alongwind concentration is equivalent to the average alongwind concentration when t_{pK} equals T_A. This complex set of relations, then, contains the computations performed in Model 3 to obtain the concentration-dosage mappings.

APPENDIX C

INPUT PARAMETERS FOR THE NASA/MSFC MULTILAYER DIFFUSION MODEL

There are two groups of input parameters for the model: the source input parameters which are vehicle and meteorologically dependent (Table C-1) and the meteorological input parameters which are strictly dependent on meteorological conditions at launch time (Table C-2). These parameters include the special set employed in the layer breakdown model — Model 4.

The source relationships given in Table C-1 are determined in reference to the stabilized ground cloud. The standard deviation of the crosswind source is

$$\sigma_{yo}\{K\} = \frac{Y\{K\}}{4.3} \quad , \tag{C-1}$$

and the standard deviation of the alongwind source is

$$\sigma_{xo}\{K\} = \frac{X\{K\}}{4.3} \quad . \tag{C-2}$$

The source strength in the Kth layer is

$$Q_K = \left(\frac{Y\{K\}\ X\{K\}}{\Sigma\, Y\{K\}\ X\{K\}}\right) \frac{Q_T}{z_{TK} - z_{BK}} \quad , \tag{C-3}$$

where $Y\{K\}$ and $X\{K\}$ describe the crosswind and alongwind dimensions of the cloud in the Kth layer, and Q_T is the total source strength in the ground cloud in units of mass.

Equations (C-1) and (C-2) are based on the assumption that the alongwind and crosswind distribution of material in each layer is Gaussian and that the visible edge of the cloud represents the point at which the concentration is one-tenth the concentration at the cloud center in the Kth layer. Equation (C-3)

assumes that the cloud is spheroidal in the plane of the horizon and that the total source strength in the Kth layer is given by the relative cloud volume in the Kth layer. Because the models require the source strength per unit height, the total source strength in the Kth layer must be divided by the depth of the layer.

The first nine meteorological parameters follow directly from the thermodynamic and kinematic profiles of the atmosphere. The remaining two parameters (layer model) are empirical atmospheric constants.

TABLE C-1. SOURCE INPUTS FOR THE MULTILAYER MODEL CALCULATIONS

Parameter		Definition
Layer Model: 1, 2, 3	Layer Breakdown Model: 4	
z_R	z_R	Reference height in the surface layer
z_{BK}	z_{BL}	Height of the layer base
z_{TK}		Height of the layer top
τ_K	τ_L	Source (cloud) stabilization time
x_{ryK}	x_{ryL}	Distance over which rectilinear lateral expansion occurs downwind from an ideal point source
$\sigma_{yo}\{K\}$		Standard deviation of the crosswind source dimension in the Kth layer
$\sigma_{xo}\{K\}$		Standard deviation of the alongwind source dimension in the Kth layer
	t^*	Time of layer breakdown
Q_K		Source strength in the layer
J		Scaling coefficient

TABLE C-2. LIST OF METEOROLOGICAL MODEL INPUTS

Parameter		Definition
Layer Model: 1, 2, 3	Layer Breakdown Model: 4	
$\bar{u}_R$	$\bar{u}_{RL}$	Mean wind speed at reference height z_R
$\bar{u}_{BK}$	$\bar{u}_{BL}$	Mean wind speed at the base of the layer
$\bar{u}_{TK}$	$\bar{u}_{TL}$	Mean wind speed at the top of the layer
θ_{BK}	θ_{BL}	Mean wind direction at the base of the layer
θ_{TK}	θ_{TL}	Mean wind direction at the top of the layer
$\sigma_{AR}\{\tau_{oK}\}$	$\sigma_{ARL}\{\tau_{oL}\}$	Standard deviation of the wind azimuth angle at height z_R
$\sigma_{ABK}\{\tau_{oK}\}$	$\sigma_{ABL}\{\tau_{oL}\}$	Standard deviation of the wind azimuth angle at the base of the layer
$\sigma_{ATK}\{\tau_{oK}\}$	$\sigma_{ATL}\{\tau_{oL}\}$	Standard deviation of the wind azimuth angle at the top of the layer
τ_{oK}	τ_{oL}	Reference time period
α_K	α_L	Lateral diffusion coefficient
$p\{K = 1\}$	$p\{L = 1\}$	Power-law exponent of the wind speed profile in the surface layer
	σ_{ERL}	Standard deviation of the wind elevation angle at height z_R
	σ_{EBL}	Standard deviation of the wind elevation angle at the base of the Lth layer
	σ_{ETL}	Standard deviation of the wind elevation angle at the top of the Lth layer
	β_L	Vertical diffusion coefficient

APPENDIX D

TOXICITY CRITERIA

A realistic evaluation of the potential hazards arising from high near-field concentrations of toxic effluents from solid rocket exhaust requires both a knowledge of the surface deposition of these effluents, which can be obtained with the NASA/MSFC Multilayer Diffusion Model (Appendix B), and toxicity criteria to evaluate the hazard from this surface deposition of effluent, which is the purpose of this discussion. The Federal Air Quality Criteria do not presently include any of the liquid or solid rocket exhaust effluents; however, the National Academy of Sciences does afford definite guidelines for the exposure to the toxic effluents associated with these exhausts. These guidelines are ecologically sound, based on the current limited knowledge of the effects of these effluents, and are the basis of the toxicity criteria that will be given [24, 25].

The primary effluents from any solid rocket exhaust are: aluminum oxide (Al_2O_3), hydrogen chloride (HCl), carbon monoxide (CO), carbon dioxide (CO_2), hydrogen (H_2), nitrogen (N_2), and water vapor (H_2O). While only the first four compounds are toxic in significant concentrations, there is always a potential hazard of suffocation from any gas which results in the reduction of the partial pressure of oxygen to a level below 135 mm Hg (18 percent by volume at STP). Oxygen level reduction does not appear to be a hazard from rocket exhaust because of the large volume of air that is entrained in these exhaust clouds; therefore, this potential hazard car be neglected in this discussion and attention can be directed to only the initial four toxic compounds. (A liquid rocket motor has only one toxic effluent — carbon monoxide.)

The exposure level for toxic effluents is divided into three categories: public exposure level, emergency public exposure level, and occuptational exposure level. The public exposure levels are designed to prevent any detrimental health effects both to all classes of human beings (children, men, women, the elderly, those of poor health, etc.) and to all forms of biological life. The emergency level is designed as a limit in which some detrimental effects may occur, especially to biological life. The occupational level gives the maximum allowable concentration which a man in good health can tolerate — this level could be hazardous to various forms of biological life.

The toxicity criteria for the toxic effluents in solid rocket exhausts are given in Table D-1. Public health levels for aluminum oxide are not given because the experience with this particulate is so limited that, at best, the industrial limits are just good estimates.

Hydrogen chloride is an irritant; therefore, the concentration criterion for an interval should not be exceeded [25]. Since hydrogen chloride is detrimental to biological life, and in view of the fact that most launch sites are encompassed by wild life refuges, the emergency and industrial criteria for hydrogen chloride are not appropriate to the ecological constraints. Because of the large volume of air entrained in the exhaust cloud, the potential hazard from carbon monoxide and carbon dioxide can be, in general, neglected.

Any detrimental health effects resulting from the combined toxicological action of these ingredients has been omitted because of a lack of knowledge in this area. However, investigations are currently underway to study this problem and to learn more about the biological effects of hydrogen chloride.

TABLE D-1. AIR QUALITY TOXICITY STANDARDS[a]

Toxic Solid Rocket Exhaust Product	Time Interval (min)	Concentration		
		Public[b]	Emergency	Occupational
Alumina (Al_2O_3)	10	5.0 mg/m^3	x	50 mg/m^3
	30	2.5 mg/m^3	x	25 mg/m^3
	60	1.5 mg/m^3	x	15 mg/m^3
	480	1.0 mg/m^3	x	10 mg/m^3
Hydrogen Chloride (HCl)	10	4 ppm	7 ppm	30 ppm
	30	2 ppm	3 ppm	20 ppm
	60	2 ppm	3 ppm	10 ppm
Carbon Monoxide (CO)	10	90 ppm	275 ppm	1000 (1500)[c] ppm
	30	35 ppm	100 ppm	500 (800)[c] ppm
	60	25 ppm	66 ppm	200 (400)[c] ppm
Dosage:		200 ppm/ time interval		
Carbon Dioxide (CO_2)	480	x	x	Average - 5000 ppm
				Peak - 6250 ppm

Note: Parts of vapor or gas per million parts of contaminated air by volume at 25° C and 760 mm Hg.

a. These values were reviewed on the phone by Ralph C. Wands, Director Advisory Center on Toxicology, National Academy of Sciences, 2101 Constitution Avenue, Washington, D. C. 20418, April 1973.

b. At these concentrations, headaches will occur along with a loss in work efficiency.

c. EPA suggests that a safety factory of ten to be applied to occupational exposure limits.

REFERENCES

1. Dumbauld, R. K. et al.: Handbook for Estimating Toxic Fuel Hazards. NASA CR-61326, Final report under Contract NAS8-21453, 1970.

2. Dumbauld, R. K.; Bjorklund, J. R.; and Bowers, J. F.: NASA/MSFC Multilayer Diffusion Models and Computer Program for Operational Prediction of Toxic Fuel Hazards. TR-73-301-02, Report under Contract No. NASA-29033, March 1973.

3. Kaufman, John W.; and Keene, Lester F.: NASA's 150-Meter Meteorological Tower Located at the Kennedy Space Center, Florida. NASA TM X-53699, January 29, 1968.

4. Susko, Michael; and Kaufman, John W.: Apollo Saturn Engine Exhaust Cloud Rise and Growth Phenomena During Initial Launch. Paper presented at MSFC's Research Achievement Review, Marshall Space Flight Center, Huntsville, Alabama, December 2, 1971.

5. Hart, W. S.: Dynamics of Large Buoyant Clouds Generated by Rocket Launches. J. Basic Eng., March 1972.

6. Briggs, G. A.: Some Recent Analyses of Plume Rise Observations. Paper presented at the 1970 International Union of Air Pollution Prevention Association, Atmospheric Turbulence and Diffusion Laboratory, National Oceanic and Atmospheric Administration, Oak Ridge, Tennessee, USA, ATDL, No. 38, 1970.

7. Hanna, Steven R.: Cooling Tower Plume Rise and Condensation. Paper presented at Air Pollution Turbulence and Diffusion Symposium, Las Cruces, New Mexico, December 7-10, 1971.

8. Smith, Michael R.; and Forbes, Richard E.: Mass-Energy Balance for an S-IC Rocket Exhaust Cloud During Static Firing. NASA CR-61357, August 4, 1971.

9. Church, H. W.: Cloud Rise from High-Explosives Detonations. TID-45000 (53rd Ed) UC-41, Health & Safety, SC-RR-68-903, Sandia Laboratories, Albuquerque, June 1969.

10. Tucker, G. L.; Malone, H. E.; and Smith, R. W.: Atmospheric Diffusion of Berryllium - Project Adobe. Report No. AFRPL-TR-70-65, Three Volumes, Director of Laboratories, Air Force System Command, July 1971.

REFERENCES (Continued)

11. Susko, Michael; Kaufman, John W.; and Hill, C. Kelly: NASA TM X-53782, October 15, 1968, pp. 146-166.

12. Thayer, Scott D.; Chandler, Martin W.; and Chu, Roland T.: Rise and Growth of Space Vehicle Engine Exhaust and Associated Diffusion Models. NASA CR-61331, July 1970.

13. Kaufman, John W.; and Susko, Michael: Review of Special Detailed Wind and Temperature Profile Measurements. J. Geophys. Res., vol. 76, no. 27, September 20, 1971.

14. Susko, Michael; and Kaufman, John W.: Exhaust Cloud Rise and Growth for Apollo Saturn Engines. J. Spacecraft and Rockets, vol. 10, no. 5, May 1974, pp. 341-345.

15. Stephens, J. Briscoe; Susko, Michael; Kaufman, John W.; and Hill, C. Kelly: An Analytical Analysis of the Dispersions for Effluents from the Saturn V and Scout-Algol III Rocket Exhausts. NASA TM X-2935, October 1973.

16. Kaufman, John W.; Susko, Michael; and Hill, C. Kelly: Prediction of Engine Exhaust Concentrations Downwind from the Delta-Thor Telsat-A Launch of November 9, 1972. NASA TM X-2939, November 1973.

17. Daniels, Glenn E.: Terrestrial Environment (Climatic) Criteria Guidelines for Use in Space Vehicle Development, 1971 Revision. NASA TM X-64589, May 10, 1971.

18. Fichtl, George H.; Kaufman, J. W.; and Vaughan, W. W.: Characteristics of Atmospheric Turbulence as Related to Wind Loads on Tall Structures. J. Spacecraft and Rockets, vol. 6, December 1969, pp. 1396-1403.

19. Fichtl, George H.; and McVehil, George E.: Longitudinal and Lateral Spectra of Turbulence in the Atmospheric Boundary Layer at the Kennedy Space Center. J. Appl. Met., vol. 9, no. 1, February 1970, pp. 51-63.

20. Climatic Atlas of the United States. U.S. Dept. of Commerce, Environmental Science Services Administration, June 1968.

REFERENCES (Concluded)

21. Laudau, L. D.; and Lifshitz, E. M.: Fluid Mechanics. Volume 6 of Course of Theoretical Physics, Pergamon Press, 1959.

22. Smith, J. W.; and Vaughan, W. W.: Monthly and Annual Wind Distribution as a Function of Altitude for Diffusion Studies. NASA Technical Report D-610, 1961.

23. Record, F. A. et al: Analysis of Tower Atmospheric Data for Diffusion Studies. NASA CR-61327, Contract No. NAS8-30503.

24. National Primary and Secondary Ambient Air Quality Standards. Environmental Protection Agency, Part II of Federal Register, vol. 36, no. 84, April 1971 (Updated November 1971).

25. Guides for Short-Term Exposures of the Public to Air Pollutants, Vol. II. Guide for Hydrogen Chloride. Committee on Toxicology of the National Academy of Sciences, National Research Council, Washington, D. C., August 1971.

26. Tyldesley, J. B.; and Wallington, C. I.: The Effect of Wind Shear and Vertical Diffusion on Horizontal Dispersion. Quart. J. Roy. Met. Soc., vol. 91, 1967, pp. 158-174.